



UNIVERSIDADE ESTADUAL DE CAMPINAS  
SISTEMA DE BIBLIOTECAS DA UNICAMP  
REPOSITÓRIO DA PRODUÇÃO CIENTÍFICA E INTELLECTUAL DA UNICAMP

**Versão do arquivo anexado / Version of attached file:**

Versão do Editor / Published Version

**Mais informações no site da editora / Further information on publisher's website:**

<https://onlinelibrary.wiley.com/doi/full/10.1111/sed.12507>

**DOI: 10.1111/sed.12507**

**Direitos autorais / Publisher's copyright statement:**

©2018 by Wiley. All rights reserved.

DIRETORIA DE TRATAMENTO DA INFORMAÇÃO


Cidade Universitária Zeferino Vaz Barão Geraldo

CEP 13083-970 – Campinas SP

Fone: (19) 3521-6493

<http://www.repositorio.unicamp.br>

## Facies and palaeosol analysis in a progradational distributive fluvial system from the Campanian–Maastrichtian Bauru Group, Brazil

ALESSANDRO BATEZELLI\* , FRANCISCO SERGIO BERNARDES LADEIRA†, DIEGO LUCIANO DO NASCIMENTO‡ and MÁRCIO LUIZ DA SILVA‡

\*Department of Geology and Natural Resources, Geosciences Institute, DGRN – IG – UNICAMP, University of Campinas, Carlos Gomes St, 250 – University City, Campinas 13083–855, São Paulo, Brazil (E-mails: abatezelli@ige.unicamp.br, alessandro.batezelli@gmail.com)

†Department of Geography, Geosciences Institute, DGRN – IG – UNICAMP, University of Campinas, Carlos Gomes St, 250 – University City, Campinas 13083–855, São Paulo, Brazil

‡Geosciences Postgraduate Program, Geosciences Institute, DGRN – IG – UNICAMP, University of Campinas, Carlos Gomes St, 250 – University City, Campinas 13083–855, São Paulo, Brazil

Associate Editor – Mariano Marzo

### ABSTRACT

The Upper Cretaceous Bauru Group in south-east Brazil consists of alluvial strata whose characteristics and distribution indicate a fluvial system developed in a semi-arid to arid climate. Sections exposed within a 90 000 km<sup>2</sup> study area in Minas Gerais State (in south-eastern Brazil) were evaluated using facies and palaeosol analysis to formulate depositional and pedogenic models that may account for geomorphic and climate features. From east to west, the study succession records a gradual decrease in grain size, an increase in the width/thickness ratio in channels, a decrease in the lateral and vertical connectivity of channel deposits, and an increase in overbank deposits. The fluvial architecture indicates a braided channel belt, ephemeral ribbon-channels, and an unconfined fluvial facies from east to west in the study area. The lateral and vertical distribution of facies, stratigraphic architecture and palaeocurrent data suggest proximal, medial and distal portions of a progradational distributive fluvial system. The sedimentary dynamics were marked by the building and abandonment of channels related to processes of aggradation, vegetation growth and palaeosol generation. Macromorphological and micromorphological analyses have identified pedological and mineralogical features that indicate an arid to semi-arid climate with a provenance from the north-eastern part of the basin (Alto Paranaíba Uplift). From the proximal to the distal portions of the distributive fluvial system, the palaeosol development is different. In the proximal portion, the palaeosols are absent or poorly developed, allowing a possible general comparison with the present soil order: Inceptisols and Aridisols. In the medial portion of the fluvial system, the palaeosols are well-developed and characterized by Bt, Btk, C and Ck horizons (Alfisols, Aridisols, Inceptisols and Entisols). Poorly drained to well-drained palaeosols from the base to the top in the distal plain (Aridisols and Inceptisols) are associated with geomorphic and hydromorphic changes in the fluvial system due to progradational evolution. The genetic relationship between the fluvial architecture and the palaeosols enhances the understanding that the sedimentation and pedogenesis that occurs in different portions of the distributive fluvial system are related to the tectonic and climatic evolution of the basin.

**Keywords** Distributive fluvial system, facies, palaeosol distribution, sedimentary and pedogenic processes.

## INTRODUCTION

With advances in the study of modern low-relief alluvial systems, large fluvial systems have been identified and are referred to in the literature as megafans, large alluvial fans, wet alluvial fans, river-dominated alluvial systems, fluvial distributary systems, distributive fluvial systems and large fluvial–fan systems (Geddes 1960; Wells & Dorr, 1987; Singh *et al.*, 1993; Stanistreet and McCarthy, 1993; DeCelles and Cavazza, 1999; Shukla *et al.*, 2001; Leier *et al.*, 2005; Fisher *et al.*, 2007; Hampton and Horton, 2007; Hartley *et al.*, 2010; Trendell *et al.*, 2013).

A distributive fluvial system (DFS) is a mega fluvial system that presents a radial distributive drainage pattern in the landscape (Hartley *et al.*, 2010). The analysis of modern sedimentary basins shows that distributive fluvial systems are the predominant fluvial form in the landscape and can comprise the most representative continental records (Weissmann *et al.*, 2010). Modern large distributive fluvial systems (more than 30 km in length) develop in all climate regimes and all sedimentary basin types.

From apex to downstream, this type of fluvial system presents a radial pattern of channels and a common decrease in channel and grain size, a higher percentage of floodplain fines and a lack of lateral channel confinement for rivers (Hartley *et al.*, 2010). Owen *et al.* (2015) characterized facies variations across the Salt Wash DFS (USA) to quantitatively test predicted trends in conceptual DFS models.

Depending on climate, and changes in accommodation space and sediment supply, the stratigraphic evolution of a DFS is highly complex, resulting in progradation, aggradation and retrogradation. Progradational architectures have been described for several fluvial sequences (e.g. Hartley, 1993; Posamentier and Allen 1999; Cain & Mountney, 2009; Trendell *et al.*, 2013; Weissmann *et al.*, 2013; Owen *et al.*, 2015; Owen *et al.*, 2017).

Despite these studies, changes in the longitudinal profiles and the autogenic processes make a clear understanding of DFS geological records

difficult. Weissmann *et al.* (2013) propose that a vertical succession through a prograding DFS has:

- 1 Distal facies at the base overlaid by proximal facies.
- 2 An increase in channel density, channel amalgamation and channel thickness up-section.
- 3 A change from poorly drained distal palaeosols to well-drained proximal palaeosols through the succession.

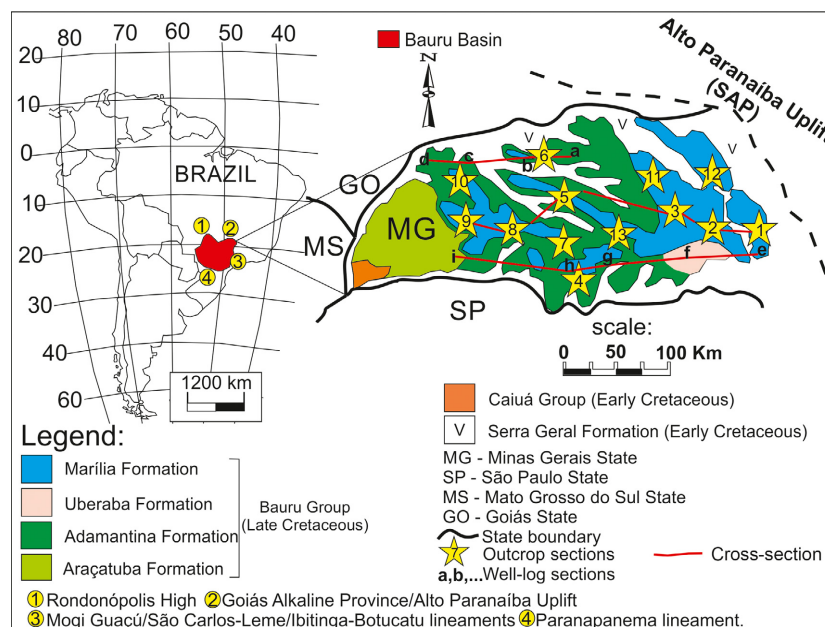
Owen *et al.* (2017) have presented quantitative documentation of the vertical trend in the prograding Salt Wash DFS and tested the conceptual model proposed by Weissmann *et al.* (2013). The aim of this study was to understand the key controlling mechanisms of the variables that can produce prograding, retrograding or aggrading trends, including changes in source area, basin and climate. These authors described vertical sections in the Salt Wash DFS and assigned facies domains based on grain size, deposit architecture and sandstone percentage.

In addition to facies and architecture analysis, the study of palaeosols has been successfully applied to fluvial deposits for stratigraphic analysis (Talbot, 1985; Wright & Marriott, 1993; Atchley *et al.*, 2004; Prochnow *et al.*, 2006; Cleveland *et al.*, 2007), landscape reconstruction (Marriott & Wright, 1993; Birkeland, 1999; Retallack, 2001; McCarthy & Plint, 2003; Miall, 2010; Kabanov *et al.*, 2010) and palaeoclimatic studies (Kraus & Hasiotis, 2006; Wright, 2007; De la Horra *et al.*, 2008; Smith *et al.*, 2008; Sheldon & Tabor, 2009; Dal'Bo *et al.*, 2009; Alonso-Zarza & Wright, 2010; Tabor & Myers, 2015).

Although palaeosols are frequently included in geological records, there are comparatively few studies that relate their evolution to the processes of building sedimentary bodies in fluvial systems (e.g. Mohindra *et al.*, 1992; McCarthy *et al.*, 1997; McCarthy *et al.*, 1999; Zaleha, 1997; Khadkikar *et al.*, 1998; Kraus, 1999; Khadkikar *et al.*, 2000; Kraus, 2002; Mack & Madoff, 2005; Jie & Chafetz, 2010; Hartley *et al.*, 2013).

In a DFS, the lateral and vertical distribution of palaeosols has been used to identify the geomorphology-based progradation hypothesis

**Fig. 1.** Lithostratigraphic map of the north-east Bauru Basin and the study area. Yellow stars indicate the outcrop section positions: 1 – Ponte Alta, 2 – Peirópolis, 3 – Uberaba, 4 – Frutal, 5 – Prata, 6 – Canápolis, 7 – Comendador Gomes, 8 – Campina Verde, 9 – Gurinhatã, 10 – Ituiutaba, 11 – BR-050, 12 – Mangabeira, and 13 – Campo Florido. Lower case letters indicate the well log section positions (a = Monte Alegre de Minas; b = Canápolis; c = Ituiutaba; d = Santa Vitória; e = Ponte Alta; f = Uberaba; g = Campo Florido; h = Comendador Gomes; and i = Honorópolis).



(Demko *et al.*, 2004; Hartley *et al.*, 2013; Weissmann *et al.*, 2013). Well-drained palaeosols occur where the water table is low, meaning that the soil is less saturated, such as those that typically occur within the proximal and medial portions of the DFS. In contrast, poorly drained palaeosols are associated with areas that have a high water table, commonly found in the distal portion of the DFS (Demko *et al.*, 2004). From the base to the top of a progradational DFS succession, the poorly drained palaeosols become less common and are replaced by better drained palaeosols (Weissmann *et al.*, 2013).

The Bauru Basin is one of the most documented and best studied sedimentary basins in Brazil, with available data including descriptions of more than 500 outcrops (350 outcrops described by Fernandes, 1998, and 150 outcrops described in Batezelli, 2003) and 1269 well logs (180 well logs presented in Paulae Silva *et al.*, 2005; 140 well logs in Batezelli, 2003; 135 well logs in Batezelli, 2015; and 814 well logs in Batezelli & Ladeira, 2016) (Fig. 1). The Bauru Basin is composed of two continental sequences deposited from the Early to Late Cretaceous (Batezelli, 2015). The Caiuá Group comprises the Goio Erê, Rio Paraná and Santo Anastácio formations and was deposited by aeolian processes in the Early Cretaceous. The Bauru Group is a record of a Late Cretaceous distributive fluvial system and is constituted by the Araçatuba, Adamantina, Uberaba and Marília formations (Batezelli & Ladeira, 2016).

The most striking features of the Bauru Group are the many palaeosol profiles associated with the fluvial deposits. In recent decades, the study of the palaeosols has been emphasized in sedimentological analysis and palaeoenvironmental evolution (e.g. Suguio *et al.*, 1975; Fernandes, 1998; Ladeira *et al.*, 2008; Dal'Bo *et al.*, 2009; Fernandes, 2010; Pereira *et al.*, 2015; Silva *et al.*, 2015; Silva *et al.*, 2016; Basilici *et al.*, 2016; Nascimento *et al.*, 2017; Silva *et al.*, 2017a,b,c).

Since 1980, the Bauru Group has been interpreted as alluvial fans and ephemeral lacustrine systems by Barcelos (1984), Fulfaro *et al.* (1994) and Fernandes & Coimbra (2000); as a braided, river-dominated alluvial system by Batezelli (2003, 2010) and Batezelli *et al.* (2007); as a megafan system by Batezelli (2015); and as a distributive fluvial system by Batezelli & Ladeira (2016) and Soares *et al.*, 2018.

Although there are depositional models that explain the evolution of the Bauru DFS, little is known about the regional characteristics. Basilici *et al.* (2016) proposed a fluvial distributive system model based on facies and palaeosols in the south-eastern part of the Bauru Basin. The model proposed is similar to other stratigraphic models (e.g. Suguio *et al.*, 1977; Etchebehere *et al.*, 1991; Batezelli, 1998; Fernandes, 1998; Fernandes & Coimbra, 2000; Dias-Brito *et al.*, 2001; Batezelli, 2003; Batezelli *et al.*, 2007; Batezelli, 2010; Fernandes, 2010; Batezelli, 2015; Fernandes & Ribeiro,

2015). Basilici *et al.* (2016) discussed the features of the genesis of palaeosols in the different areas of the distributary fluvial system, presenting the Echaporã pedotype as a reference profile, and interpreted the environmental evolution of the basin. Although the environmental model is compatible with other models for the basin, the profiles presented by these authors are unfortunately not correct: the succession of horizons A–Bw–Btk–C (Echaporã pedotype), Bw1–Bw2–Btk, Bw–Btk–C and A/Bw–Btk–C (figs 9, 12, 14 and 15 of Basilici *et al.*, 2016) is incompatible with the evolution of soils. As the soil evolves from the top to the base, it is impossible for the less evolved Bw horizon to occur above the more evolved Bt horizon (Soil Survey Staff, 2006).

In this way, a detailed analysis of facies, palaeosols and stratigraphic architecture is presented in the north-eastern part of the Bauru Basin in order to construct an evolutionary model that integrates depositional and pedogenetic characteristics in the DFS. Based on facies and architectural element analysis of the 61 outcrops in an area of 90 000 km<sup>2</sup>, a braided channel belt, ephemeral ribbon channels and unconfined fluvial facies that correspond to the proximal, medial and distal domains of the DFS, respectively, were identified. Lateral and vertical changes in facies association, stratigraphic architecture, and palaeocurrent and petrography data indicate a source area in the north-eastern Bauru Basin and a progradational pattern basinward in the west. The macromorphology and micromorphology identified changes from well-drained to poorly drained palaeosols in all of the study area, corresponding to those reported in distributive fluvial systems by Hartley *et al.* (2013) and Weissmann *et al.* (2013). By analysing the relationship between facies and palaeosols, a palaeogeographic model of the Late Cretaceous Bauru distributive fluvial system, relating its evolution to tectonic and climate events, was elaborated.

## GEOLOGICAL SETTING

### General

The Bauru Basin is an intracratonic basin that is elongated NNE and occupies 330 000 km<sup>2</sup> in south-eastern Brazil. Its origin is attributed to flexural subsidence occurring south-west of the Alto Paranaíba Uplift (SAP) after the magmatic

activity related to the Trindade Mantle Plume (Gibson *et al.*, 1995) during the Late Cretaceous (Fig. 1).

The substrate of the basin is partly formed by the Caiuá Group sandstone (Lower Cretaceous) and the Serra Geral Formation basalt (São Bento Group – Lower Cretaceous), rearranged in an elongated north-east/south-west trending depression. The sedimentation was controlled by successive uplifts of the SAP in the northern and north-eastern portions. The basin records continental sedimentation (Bauru Group) with a maximum preserved thickness on the order of 300 m, composed of mudstone and very fine sandstone at the base (Araçatuba Formation), grading to fine to medium-grained sandstone in the medial portion (Adamantina and Uberaba formations) and fine to coarse-grained, in addition to conglomeratic, sandstone at the top (Marília Formation) (Fig. 2).

The present limits of the Bauru Basin are essentially erosive and/or tectonic and are outlined by the Rondonópolis High (Coimbra, 1991) to the north-west, the Goiás Alkaline Province/Alto Paranaíba Uplift (Hasui & Haralyi, 1991) to the NNE, the Mogi Guaçu River (Coimbra *et al.*, 1981), and the São Carlos–Leme and Ibitinga–Botucatu lineaments (Riccomini, 1997) to the east, and the Paranapanema lineament (Fulfaro, 1974) to the south and south-east. The limit is diffuse at the western margin because of the large area of Cenozoic fluvial deposits associated with the Paraná River plain (Fig. 1).

The erosive processes responsible for the development of the present Bauru Basin boundaries are related to the Late Cretaceous and Tertiary tectonic restructuring event, which was marked by the uplift of the Serra do Mar mountain range (SM) and the Alto Paranaíba Uplift (SAP), and by the faulting related to the genesis of the Pantanal Basin on the western border in Mato Grosso State. The basement of the Bauru Basin is constituted by the Early Cretaceous Serra Geral Formation basalts (Batezelli, 2015).

### Stratigraphic sequences

The Bauru Basin sedimentary record presents two major unconformity-bounded second-order depositional sequences (*sensu* Mitchum *et al.*, 1977): Sequence 1 (Caiuá Group) and Sequence 2 (Bauru Group: Araçatuba, Adamantina/Uberaba and Marília formations; Batezelli, 2015). Sequence 2 can be divided into two third-order

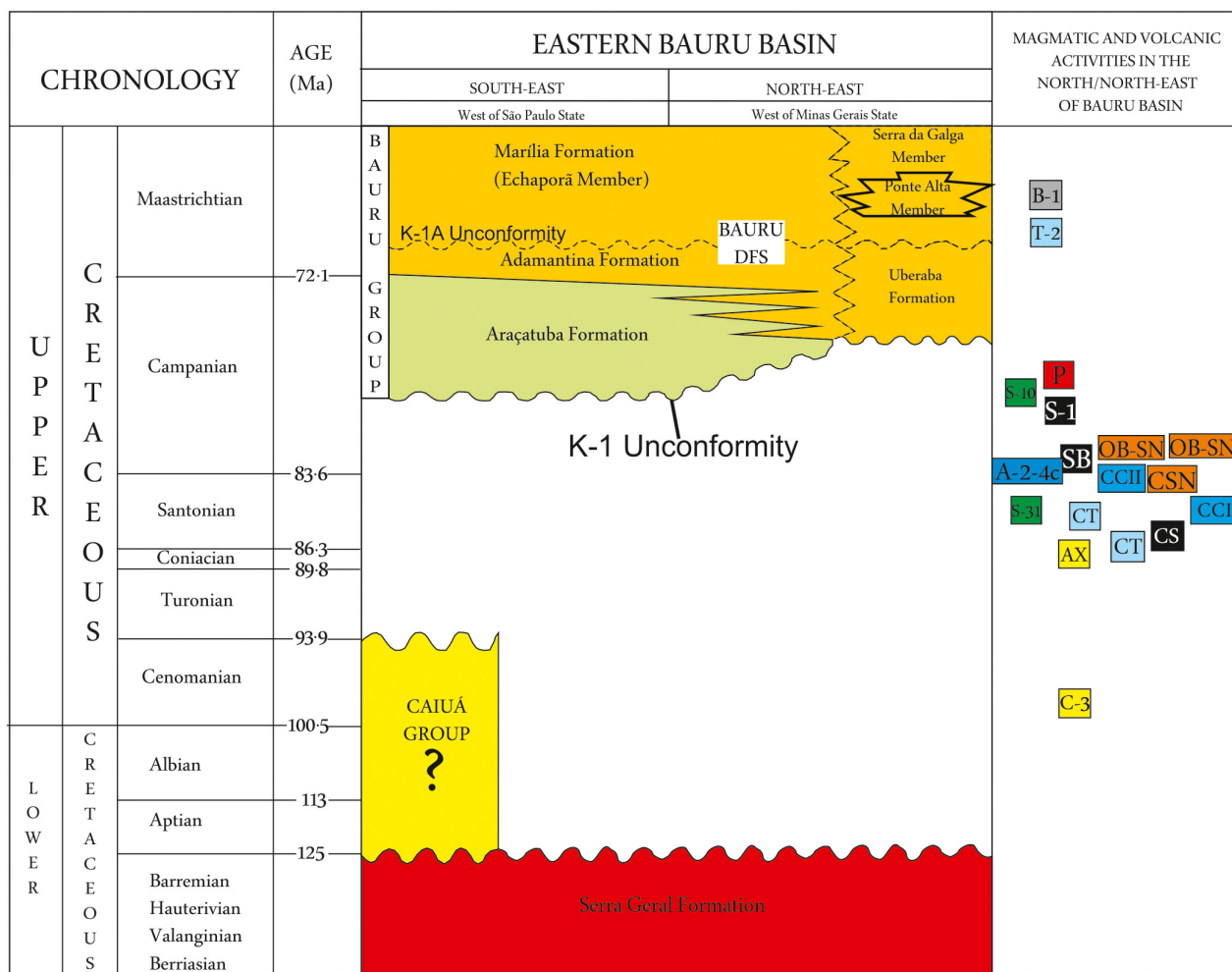


**Fig. 2.** Chronostratigraphic chart of the Cretaceous sequence in southern Brazil, based on Amaral *et al.*, 1967 (sample CSN); Hasui & Cordani, 1968 (samples AX, C-3, S-10, S-31, A-2-4c, OB-SN, SB, S-1, P, T-2 and B-1); Sonoki & Garda, 1988 (samples CT, CS and CCI); Machado Junior, 1992 (sample CCI); Guimarães *et al.*, 2012, and Fragoso *et al.*, 2013 (Pterosaurs); Gobbo-Rodrigues, 2001, and Dias-Brito *et al.*, 2001 (Ostracods); Santucci & Bertini, 2001, and Martinelli *et al.*, 2011 (Allosaurus) (modified after Batezelli, 2015).

depositional sequences (Sequences 2A and 2B), bounded by the unconformity K-1A.

Unconformably overlying the Early Cretaceous Serra Geral basalts (unconformity K-0) and occurring at the base of the Bauru Basin, Sequence 1 is constituted by the Draa facies association of the Caiuá Group (Figs 1 and 2; Batezelli, 2015).

Sequence 2A unconformably overlies the aeolian deposits of the Caiuá Group and is constituted by sandy mudstone and mudstone at the base (lacustrine facies association – Araçatuba Formation) and sandstones to mudstones in the medial to top portions (fluvial facies association – Adamantina/Uberaba formations; Batezelli, 2015). The boundary of the sequences is marked by an unconformity that

separates the aeolian sandstones (unconformity K-1) from the lacustrine/fluvial deposits. The basal contact of the lacustrine facies association deposits is discordant both in relation to the Serra Geral Formation basalts and the aeolian sandstones (Fig. 2). The upper and lateral contacts are gradational and interfingering with the fluvial facies association (Adamantina and Uberaba formations, respectively; Fig. 2; Batezelli, 2015).

Overlying Sequence 2A, Sequence 2B consists of sandstones, conglomerates and palaeosols from the alluvial facies association (Marília Formation). The basal contact of Sequence 2B is either gradational or abrupt (unconformity K-1A) with Sequence 2A (Batezelli, 2015). The unconformity K-1A, correlative across the study area

both in outcrops and in well logs, was most probably associated with the last renewal of the source area in the northern and north-eastern Bauru Basin in the early Maastrichtian (Fig. 2). This event has eroded part of the pre-Maastrichtian deposits mainly in the north and north-eastern basin where the Serra Geral basalts were exposed. The uplifts in the north and north-eastern parts of the Bauru Basin, in addition to erosive events, were responsible for the increase in sediment supply, promoting changes in the depositional environments (Batezelli, 2015).

### Chronostratigraphy

Based on the integration of the palaeontological data (Guimarães *et al.*, 2012; Fragoso *et al.*, 2013; Gobbo-Rodrigues, 2001; Dias-Brito *et al.*, 2001; Santucci & Bertini, 2001; Martinelli *et al.*, 2011) and stratigraphic information (Batezelli, 2010, 2015), as well as correlations with tectonic and magmatic events (Amaral *et al.*, 1967; Hasui & Cordani, 1968; Sonoki & Garda, 1988; Machado Junior, 1992) that occurred in the northern and north-eastern portions of the Bauru Basin, the Bauru Group is assigned to the Campanian–Maastrichtian age (Fig. 2).

### Bauru distributive fluvial system

The Bauru DFS was deposited from the Campanian to Maastrichtian in the northern and north-eastern portions of the Bauru Basin (Batezelli & Ladeira, 2016) (Fig. 2). During the Late Cretaceous, uplifts related to the passage of the central-eastern portion of South America over the Trindade mantle plume (Gibson *et al.*, 1995) generated highlands responsible for creating a large fluvial system in the Bauru Basin. It has been suggested that the apex is in the area named the Alto Paranaíba Uplift (SAP; Hasui & Haralyi, 1991) in western Minas Gerais (Fig. 1). These highlands spanned the northern limits of São Paulo and Minas Gerais through Goiás, Mato Grosso and Rondonia states, extending north-westward to eastern Bolivia, and have been important interfluvial regions since the Late Cretaceous.

The evolution of the SAP has resulted in variable flexural subsidence rates basinward, as well as changes in the sedimentary environments. Bauru Group thickness maps published in Batezelli (2003) attest to the prograding fluvial systems from the north/north-east to the south/south-west in the basin.

In this paper, the Bauru DFS corresponds lithostratigraphically to the Uberaba, Adamantina and Marília formations (Figs 1 and 2). The Uberaba and Adamantina formations consist of low-sinuosity amalgamated braided fluvial channels (Uberaba Formation) varying with a complex of multi-lateral and single-storey channels (Adamantina Formation) separated by floodplain deposits downstream (corresponding to medial and distal parts of the system). The Marília Formation comprises gravelly to sandy amalgamated fluvial channel deposits interlayered with carbonate palaeosols, overlying the fluvial facies of the Uberaba and Adamantina formations (Figs 1 and 2) (Batezelli, 2010; Batezelli, 2015; Batezelli & Ladeira, 2016).

These characteristics, coupled with a dispersive palaeocurrent pattern, allowed Fulfaro & Perinotto (1996) and Batezelli (2003) to interpret the Bauru Group as a braided river-dominated alluvial system (*sensu* Stanistreet & McCarthy, 1993) and, later, Batezelli (2015) and Batezelli & Ladeira (2016) interpreted it as a megafan and a DFS, respectively.

The term 'Bauru DFS' includes all three formations to emphasize that these formations are a single depositional system. Because of post-Cretaceous erosion, the geological record is relatively thin for its size and has low overall accumulation rates. In São Paulo State, the Bauru DFS is 300 m thick, while in the Uberaba area in Minas Gerais State, its deposits are up to 70 m thick. (Fig. 1).

### STUDY AREA, SAMPLING AND METHODS

The study area is in western Minas Gerais State in south-eastern Brazil (Fig. 1). This work consists of a description of facies and palaeosols within an area of *ca* 90 000 km<sup>2</sup> from a total of 61 outcrops.

This paper presents information on columnar sections from 10 outcrops described in detail (for a total of 565 m of sections), where it was possible to recognize the association of facies, palaeosols and depositional architectures. Facies characterization combining field work and the petrographic analysis of samples was performed, focusing on the texture, colour and sedimentary structures, as well as the interpretation of the depositional and diagenetic processes (Table 1).

The depositional architectures were defined using photomosaic bi-dimensional sections

**Table 1.** Facies described in the study area (based on Miall, 1985).

Facies	Characteristic
Gt	Clast-supported conglomerates constituted by pebbles of quartz, clay and carbonate fragments. These facies can form metric lenticular or tabular bodies, or centimetric layers in the base of fining-upward cycles. Frequently, this facies exhibits trough cross-stratification or normal grading
Gm	Sandy matrix-supported conglomerates, constituted by angular to subangular pebbles of quartz, clay and carbonate fragments. This facies occurs as lenticular bodies or fill small channels
St	Fine to coarse-grained sandstone with trough cross-stratification, forming tabular bodies with thicknesses varying from 1.0 to 2.30 m. The grains are sub-angular to sub-rounded and the trough cross-stratifications vary from medium to large-scale (up to 3 m)
Gc	Conglomerates cemented by CaCO <sub>3</sub>
Sc	Litho-arenite cemented by CaCO <sub>3</sub>
Sm	Fine to coarse, massive sandstone, with sub-angular to sub-rounded grains, and thicknesses varying from 1.0 to 1.5 m
Fm	Reddish, massive mudstone with carbonate nodules and root marks. In some parts of the study area the mudstone is laminated and intercalated with gypsite layers. Root marks up to 50 cm are vertical and filled by sand and or calcium carbonate. This facies occurs in tabular layers varying from 50 cm to 2 m thick
Srh	Rhythmic succession of red muddy medium to very fine sandstones that exhibit fining-upward cycles; they subordinately exhibit cross-lamination, ripple marks, dish structures and convoluted folds

**Table 2.** Facies, architectural elements and facies association of the study area (based on Miall, 1985).

Facies	Architectural elements	Facies association
Gt, Gm, St, Gc, Sc	CH – Channel	Braided channel belt
Gm, Gt, St, Sm	CH – Channel SB – Sand bars	Ephemeral ribbon channels
Fm, St	OF – Overbank deposits Aeo – Aeolian deposits	
Srh	LS – Laminated sand sheets	Unconfined fluvial
Gm, St, Sm, Fm	CH – Channel OF – Overbank deposits	

according to the method of Miall (1985). Fluvial architectural elements such as channels (CH element), laminated sand sheets (LS element), overbank deposits (OF element) and sand bars (SB element) were identified. Subordinate aeolian deposits (Aeo element) occur interlayered with the above elements. These architectural elements allowed the identification of the fluvial pattern from east to west in the study area, delimiting the areas of the braided channel belt, ephemeral ribbon channels and unconfined fluvial channels (Table 2).

In addition to the 61 outcrop descriptions, 35 well logs obtained from the Sanitation Company of Minas Gerais State (COPASA) were used to calculate the percentages of sand and clay in the Upper Cretaceous Bauru DFS, which served as the basis for the facies map of the study area (Tables 3 and 4). Three east–west stratigraphic sections were elaborated based on outcrops and well logs. The integration of the stratigraphic sections and the maps of the facies and palaeocurrents allowed the reconstruction of the progradational distributive fluvial system, delimiting three distinct areas: proximal, medial and distal.

Distributive fluvial systems are characterized by radial channel patterns, a decrease in channel size downstream with an increase in floodplain deposits, a decrease in grain size downstream, and changes from amalgamated channel deposits in proximal areas to smaller fixed channels in distal areas (Hirst 1991; Stanistreet & McCarthy 1993; Nichols & Fisher 2007; Cain & Mountney 2009; Hartley *et al.*, 2010; Weissmann *et al.*, 2010, 2013). In the present study, the radial channel pattern was identified by palaeocurrent data, while the other parameters were based on qualitative analysis of the facies.

Palaeosol recognition was carried out using Soil Survey Staff (2006) criteria based on macromorphological features, such as bioturbation, pedogenic structures, horizons, colour, nodules,



**Table 3.** Lithological classification based on sandstone/mudstone rate of the stratigraphic sections described in the study area.

Stratigraphic Sections	Coordinates		Sandstone (%)	Mudstone (%)	Sandstone/Mudstone rate	Facies classification
	Longitude	Latitude				
AS-01	826.681	7815.368	100	0	>1	Sandstone
AS-02	822.371	7812.470	97,77	2,22	44,04	Sandstone
AS-03	822.306	7813.450	100	0	>1	Sandstone
AS-04	822.045	7814.691	50	50	1	Sandstone
AS-05	801.631	7859.821	85	15	5,66	Sandstone
AS-06	807.600	7816.450	99,56	0,43	231,53	Sandstone
AS-07	836.320	7827.819	100	0	>1	Sandstone
AS-08	833.526	7823.193	100	0	>1	Sandstone
AS-09	830.897	7821.211	100	0	>1	Sandstone
AS-10	816.257	7818.165	100	0	>1	Sandstone
AS-32	744.074	7815.648	100	0	>1	Sandstone
AS-36	837.849	7829.382	100	0	>1	Sandstone
AS-37	850.120	7818.277	100	0	>1	Sandstone
AS-38	835.353	7816.616	88,34	11,66	7,57	Sandstone
AS-62	807.600	7816.450	88,38	11,62	7,60	Sandstone
AS-63	815.580	7810.768	96,4	3,6	26,77	Sandstone
AS-64	807.896	7828.276	100	0	>1	Sandstone
AS-65	808.152	7830.995	100	0	>1	Sandstone
AS-66	806.545	7832.683	100	0	>1	Sandstone
AS-67	807.250	7851.273	100	0	>1	Sandstone
AS-68	805.047	7846.326	100	0	>1	Sandstone
AS-69	828.429	7830.212	100	0	>1	Sandstone
AS-70	785.764	7833.173	95	5	19	Sandstone
AS-71	780.933	7826.712	100	0	>1	Sandstone
AS-72	811.753	7830.967	100	0	>1	Sandstone
AS-73	849.324	7879.815	100	0	>1	Sandstone
AS-13	805.694	7838.007	100	0	>1	Sandstone
AS-18	620.239	7860.005	100	0	>1	Sandstone
AS-19	624.582	7863.649	100	0	>1	Sandstone
AS-20	626.181	7862.716	100	0	>1	Sandstone
AS-21	631.316	7866.523	0	100	0	Mudstone
AS-23	620.070	7878.836	97,6	2,4	40,66	Sandstone
AS-24	647.018	7851.521	0	100	0	Mudstone
AS-25a	647.502	7853.639	100	0	>1	Sandstone
AS-25b	647.180	7853.549	90	10	9	Sandstone
AS-26	644.945	7858.610	100	0	>1	Sandstone
AS-28	735.773	7855.791	0	100	0	Mudstone
AS-31	637.471	7801.296	0	100	0	Mudstone
AS-39	642.372	7701.321	80	20	4	Sandstone
AS-40	544.098	7715.762	0	100	0	Mudstone
AS-41	491.721	7722.304	0	100	0	Mudstone
AS-42	461.501	7760.474	0	100	0	Mudstone
AS-43	484.687	7820.913	0	100	0	Mudstone
AS-44	455.634	7855.722	40	60	0,66	Mudstone
AS-45	422.121	7882.506	100	0	>1	Sandstone
AS-46	432.444	7887.527	100	0	>1	Sandstone
AS-47	444.874	7893.562	100	0	>1	Sandstone
AS-48	447.024	7897.872	100	0	>1	Sandstone
AS-49	555.100	7995.851	100	0	>1	Sandstone
AS-50	561.788	7973.425	0	100	0	Mudstone
AS-51	561.398	7970.845	91,94	8,06	11,40	Sandstone
AS-52	654.048	7924.947	100	0	>1	Sandstone
AS-53	554.179	7764.982	32,92	67,08	0,49	Mudstone
AS-54	548.829	7761.520	39,63	60,37	0,65	Mudstone

Table 3. (continued)

Stratigraphic Sections	Coordinates		Sandstone (%)	Mudstone (%)	Sandstone/Mudstone rate	Facies classification
	Longitude	Latitude				
AS-55	604-436	7739-572	0	100	0	Mudstone
AS-56	602-062	7730-270	0	100	0	Mudstone
AS-57	599-672	7717-894	0	100	0	Mudstone
AS-58	655-650	7885-770	23,08	76,92	0,30	Mudstone
AS-59	672-150	7892-287	0	100	0	Mudstone
AS-60	673-600	7879-568	0	100	0	Mudstone
AS-61	700-250	7910-180	0	100	0	Mudstone

calcium carbonate cementation, transition and mottling, described according to the *Field Book for Describing and Sampling Soils* (Schoeneberger *et al.*, 2012). Although palaeosol profiles were described in all study areas, three reference sections (Sections 3, 8 and 9; Fig. 1) were measured in detail (Uberaba, Campina Verde and Gurinhata palaeosol sequences). These sections presented the relationship between deposits and palaeosols, which allowed an understanding of sedimentation and pedogenesis processes. Palaeosol classifications were based on those of the USDA (Soil Survey Staff, 2006) using micromorphology and geochemical analysis.

Thin sections were made from more than 50 samples of the sandstones and palaeosols. The petrography of the sandstones was described to identify the provenance of the deposits based on mineral content, texture and maturity. Micromorphological analysis of palaeosols based on Stoops *et al.* (2010) identified pedogenic features such as fabric, nodules, carbonate cementation, alluvial clay and coatings, among other characteristics related to the genesis of palaeosols. The integration of facies and palaeosol analysis allowed the creation of a palaeogeographic model of the Bauru DFS.

## RESULTS

### Facies and architectural elements

Based on facies analysis, three facies associations were identified in the study area: braided channel belt, ephemeral ribbon channels and unconfined fluvial facies associations.

#### *The braided channel belt facies association*

This facies association consists of clast-supported conglomerates (Gt facies) and whitish,

fine to coarse-grained calciferous pebbly sandstones (Gm facies), reaching a maximum thickness of 60 m (Fig. 3). Conglomeratic sandstones grade into coarse-grained sandstones with trough cross-stratification (St facies; Fig. 4). These facies are poorly sorted and the clasts are sub-angular to sub-rounded (Fig. 4), consisting of basalt, quartz, quartzite and flint with diameters varying from 5 to 15 cm.

In the eastern study area (Ponte Alta, Peirópolis and Uberaba cities), the Gt, Gm and St facies occur in cycles fining-upward, forming lenticular and amalgamated bodies up to 1 m thick and limited by second-order surfaces. Third-order surfaces are continuous and slightly concave up, bounding these facies associations in a succession of channel deposits with thicknesses of up to 30 m (CH element; Fig. 4).

One of the most striking characteristics of the sandstones in the study area is their range in cement carbonate content. Because of the different cement contents, the rocks can be classified as carbonate litharenites and carbonate conglomerates (50% in carbonate matrix) (Sc and Gc facies, respectively). These carbonates are fine to coarse-grained, massive and poorly sorted, forming lenticular bodies 8 m thick and extending for hundreds of kilometres, limited at the base and the top by third-order surfaces (CHc element). Because of the high contents of CaCO<sub>3</sub>, these occurrences are exploited as raw material for Portland cement and as a soil corrective in the Uberaba and Uberlândia regions (Fig. 3).

*Petrography.* The sandstones vary from fine to coarse-grained and are poorly sorted, with clasts ranging from angular to sub-angular, and the packing is soft with floating contacts. Quartz occurs in *ca* 50% of the sandstones and is the

**Table 4.** Lithological classification based on the sandstone/mudstone rate of the well-log of the study area.

Well-log	Coordinates		Sand thickness (m)	% of sand	Mud thickness (m)	% of mud	Sand/mud rate	Classification
	E	W						
Ara-02	799.750	7931.242	20	44.44	25	55.56	0.79	Muddy
CF-01	754.093	7812.005	53	99	0	1	99	Sandy
CF-02	754.520	7812.833	10	99	0	1	99	Sandy
Can-03	694.158	7922.047	60	99	0	1	99	Sandy
Car-01	532.130	7821.840	0	1	105	99	0.01	Muddy
Car-08	519.799	7823.398	100	99	0	1	99	Sandy
Cen-01	690.416	7942.901	0	1	15	99	0.01	Muddy
Cen-02	690.305	7944.550	0	1	15	99	0.01	Muddy
Cen-03	689.586	7944.297	0	1	20	99	0.01	Muddy
CG-01	709.240	7821.888	100	99	0	1	99	Sandy
CG-02	700.480	7821.884	36	99	0	1	99	Sandy
ES-01	823.926	7929.130	86	99	0	1	99	Sandy
Fru-01	715.127	7785.006	0	0	0	0	0	–
Gu-01	627.853	7875.192	70	90.9	7	9.1	10.97	Sandy
Hon-01	601.390	7833.596	0	0	18	100	0	Muddy
Hon-02	603.843	7836.803	27	28.42	68	71.58	0.39	Muddy
Itur-01	568.810	7840.503	35	38.88	55	61.12	0.63	Muddy
Itur-02	569.430	7840.383	178	99	0	1	99	Sandy
Itur-03	583.360	7818.500	88	46.31	102	53.69	0.86	Muddy
LDo-01	548.600	7846.808	0	1	55	99	0.01	Muddy
LDo-02	549.703	7846.600	8	44.44	10	55.56	0.79	Muddy
Pra-03	682.939	7836.424	0	1	15	99	0.01	Muddy
Ped-02	869.945	7873.769	0	0	0	0	0	–
Rom-01	868.307	7886.120	62	99	0	1	99	Sandy
Sac-02	865.069	7812.041	0	0	0	0	0	–
SaV-03	601.653	7905.103	10	50	10	50	1	Sandy
SaV-06	604.031	7905.097	7	99	0	1	99	Sandy
SaV-07	602.467	7905.217	15	99	0	1	99	Sandy
SFS-01	628.374	7802.970	0	0	0	0	0	–
Uba-01	809.334	7813.353	63	86.3	10	13.7	6.29	Sandy
Uba-02	824.559	7815.563	50	71.42	20	28.58	2.49	Sandy
Uba-03	811.697	7813.310	0	1	60	99	0.01	Muddy
Uba-04	824.193	7813.196	0	1	35	99	0.01	Muddy
Uba-05	826.900	7814.059	0	1	80	99	0.01	Muddy
Ver-02	779.222	7824.710	7	99	0	1	99	Sandy

main detrital phase of the rock. Its forms are both polycrystalline and monocrystalline, with undulating extinction.

As noted, the carbonate occurs as a cement in a large range of concentrations in conglomerates and sandstones. Due to substitution of the framework grains by carbonate cement, it is difficult to observe the original shapes of the grains in some of the samples.

In thin section, calcite and dolomite are the main carbonate minerals (Fig. 5A and B). The calcite occurs with micrite-dominated alpha fabric and replaces terrigenous clasts mainly at the edges of the grains (Fig. 5C). It is common to observe calcite spar and barite coats surrounding the siliciclastic grains (Fig. 5D).

Rock fragments make up *ca* 30% of the analysed samples. Lithic fragments consist of quartzite (Fig. 5D). The rock fragments have much larger dimensions than the other components of the framework. Feldspars compose *ca* 15% of the composition of the rock framework and include mainly alkali feldspars with subordinate plagioclase. The mineralogical composition is quite varied, and modal analysis data in the diagram by McBride (1963) classifies the samples as feldspathic litharenites and litharenites (Fig. 6).

#### *Ephemeral ribbon channels facies association*

This facies association consists of massive and stratified sandstone (Sm and St facies), clast-



**Fig. 3.** Stratigraphic Section 1 and the braided channel belt facies association. (A) Panoramic view of the braided channel belt facies association in Lafarge Quarry (Ponte Alta – MG). (outcrop is 60 m high) (B) Whitish, fine to coarse-grained calciferous pebbly sandstones (facies Gm) (outcrop is 9 m high). (C) Detail of the massive carbonates (CH element). Coin for scale is 3 cm in diameter.

supported conglomerate (Gm and Gt facies), mudstone (Fm facies) and palaeosols (P; Fig. 7).

The conglomerates (Gm) are matrix-supported and comprise fragments of quartz, clay and carbonate with diameters ranging from 2 to 10 cm (Fig. 7A). This facies forms lenticular or tabular bodies in the base of fining-upward cycles, and its thickness varies from a few centimetres to 1 m. Frequently, these facies exhibit trough cross-stratification or normal grading (Gt facies; Fig. 7B).

The sandstone with trough cross-stratification (St facies) and massive sandstone (Sm facies) form tabular bodies with thicknesses varying from 1.0 to 2.30 m. The grain size is fine to coarse, with sub-angular to sub-rounded clasts, with medium to large-scale trough cross-

stratification (up to 3 m). These facies are associated with conglomerate in fining-upward cycles (Fig. 7C) or aeolian deposits.

The mudstone facies (Fm facies) occurs in tabular layers up to 2 m thick, composed of reddish massive mudstone with carbonate nodules and root marks (Fig. 7D).

The architectural elements identified in this portion of the study area are ribbon channels (CH element), amalgamated sand bars (SB element), overbank deposits (OF element) and aeolian deposits (Aeo element; Fig. 8).

Channel elements (CH) provide the largest architectural geometry in this portion of the study area. These channels have lenticular shapes with slightly concave-up bases, are dozens of metres in length and 1.5 m thick, and are

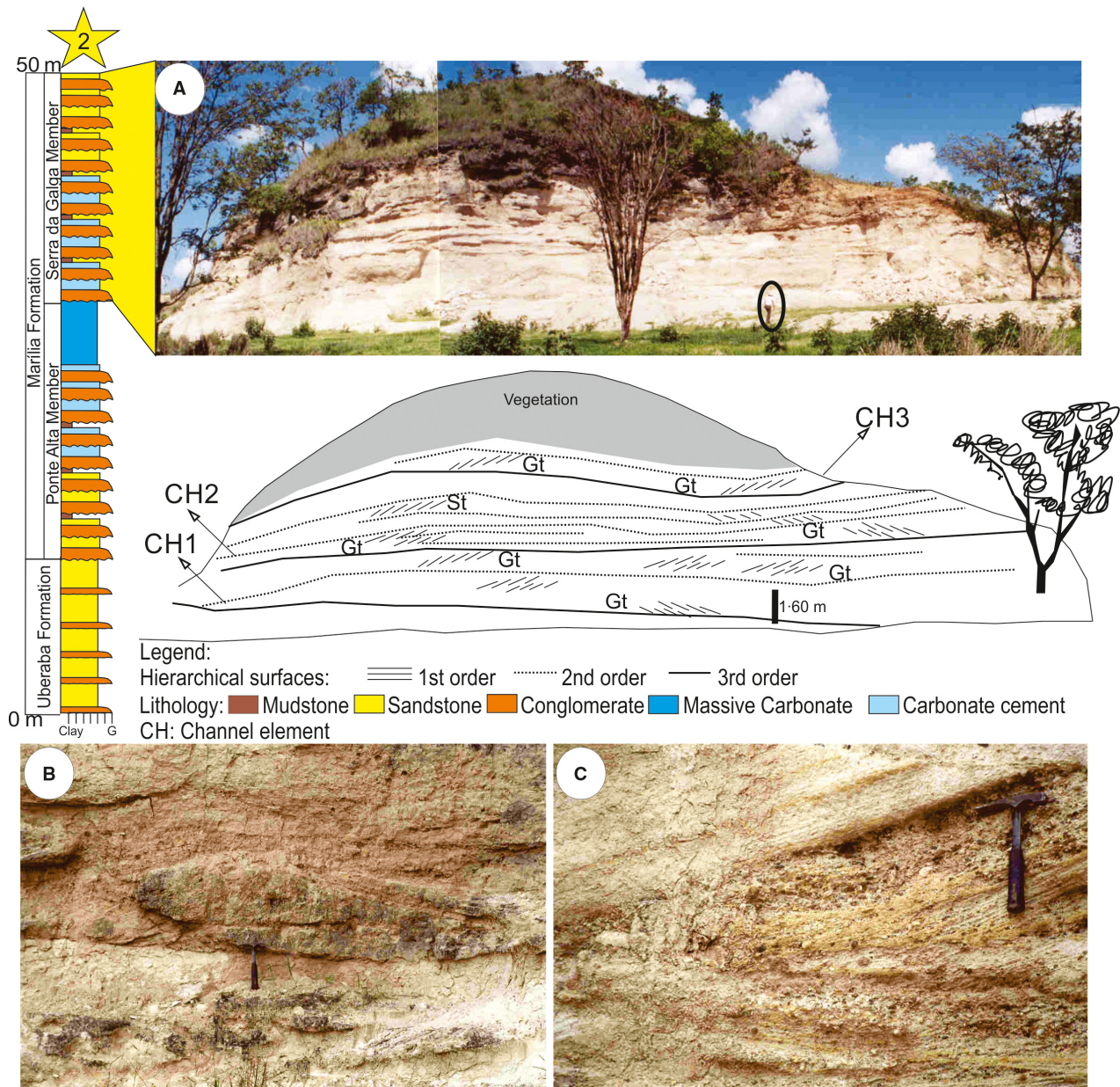


**Fig. 4.** Stratigraphic Section 2 and the braided channel belt facies association. (A) Panoramic view and architectural elements (Peirópolis – MG). Person for scale is *ca* 1.8 m tall. (B) Detail of sand bars. (C) Detail of the conglomerate with trough cross-stratification. Hammer for scale is 40 cm long.

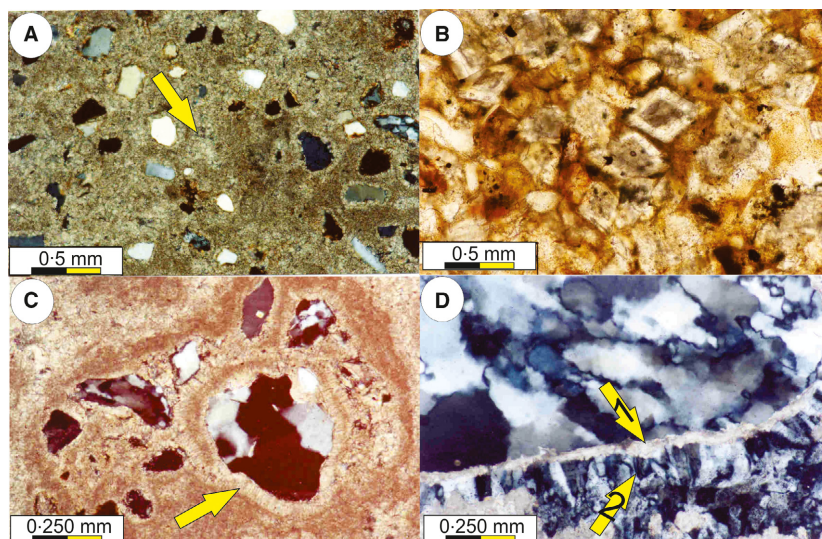
constituted by Gm, Gt, St, Sm and palaeosols. Most of the sand deposits in CH elements are composed of lenticular sand bars (SB element) reaching a maximum of 15 m in length.

Two other elements are identified in this part of the study area: overbank and aeolian deposits (OF and Aeo elements). These architectural elements are isolated at the bases of the sections and consist of mudstones (Fm facies) and large-scale trough cross-stratified sandstone (St facies), respectively.

#### *Unconfined fluvial facies association*

This facies association consists of medium to very fine-grained silty sandstone in tabular strata up to 70 cm thick, having parallel lamination in rhythmic cycles that fine upward and carbonate cementation (Srh facies). Massive and stratified sandstones (Sm and St facies), clast-supported and matrix-supported conglomerates (Gm facies), mudstone (Fm facies) and palaeosols (P) are frequent in this portion of the area (Fig. 9).

**Fig. 5.** (A) Soft packing and floating contacts in carbonatic immature sandstone. The yellow arrow indicates micrite cement constituting the alpha fabric. (B) Detail of the dolomite cement and coats of iron oxide. (C) Quartzite fragment replaced by carbonate and calcite spar surrounding quartzite fragment (yellow arrow). (D) Quartzite fragment with calcite spar (yellow arrow '1') and barite coats (yellow arrow '2').



The Srh facies is composed of a rhythmic succession of red muddy medium to very fine-grained sandstones that exhibit fining-upward (Fig. 9A and B); they subordinately exhibit cross-lamination, ripple marks, dish structures and convoluted folds. Associated with fining-upward cycles, clast-supported conglomerate layers occur up to 1 m thick (Gm facies). These conglomerates occur as lenticular bodies or fill small channels and consist of angular and sub-angular clay pebbles (Fig. 9C).

The sandstone with trough cross-stratification (St facies) and massive sandstone (Sm facies) form tabular bodies with thicknesses from 1.0 to 1.5 m. The grain size is fine to coarse, with sub-angular to sub-rounded clasts and small-scale trough cross-stratification (up to 1.5 m).

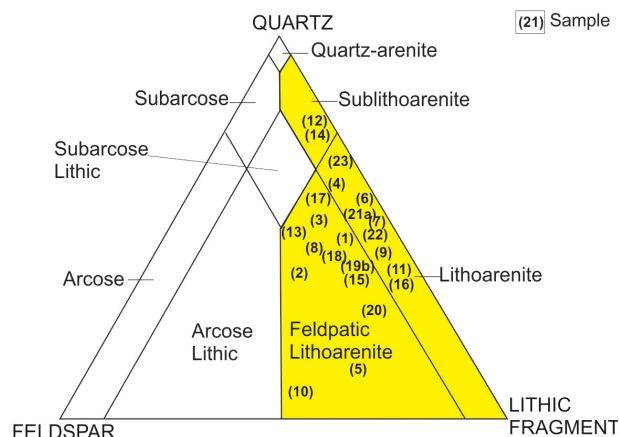


**Fig. 6.** Petrographic classification (McBride, 1963) of the braided channel belt facies association (Batezelli, 2003).

The mudstone facies (Fm facies) occurs in tabular layers up to 0.50 cm thick, constituted by reddish laminated mudstone with gypsum layers, carbonate nodules and root marks. Root marks up to 50 cm are vertical and filled by sand and/or calcium carbonate.

The architectural elements identified in this portion of the study area are laminated sand sheets (LS element), channel deposits (CH element) and palaeosols. Laminated sand sheets (LS element) are the main architectural element in this area; they consist of rhythmite deposits (Srh facies), mudstones (Fm facies) and intraformational conglomerates (Gm facies). This element has a tabular shape and is hundreds of metres in length and more than 20 m thick.

Channel deposits (CH element) overlie the LS element with slightly concave-up bases, are dozens of metres in length and 15 m thick and are constituted by Gm, St, Sm and palaeosols. The sand deposits in the CH elements consist of amalgamated sand bars (SB element) up to 6 m thick and 10 m in length.

### Palaeosols

Whilst previous studies of Bauru DFS palaeosols have been undertaken (e.g. Suguio *et al.*, 1975; Fernandes, 1998; Ladeira *et al.*, 2008; Dal'Bo *et al.*, 2009; Fernandes, 2010; Pereira *et al.*, 2015; Silva *et al.*, 2015; Silva *et al.*, 2016; Nascimento *et al.*, 2017; Silva *et al.*, 2017a,b,c), little is known about their lateral and vertical distributions or their stratigraphic meaning. Associated with the facies and architectural elements, palaeosol profiles with different degrees of

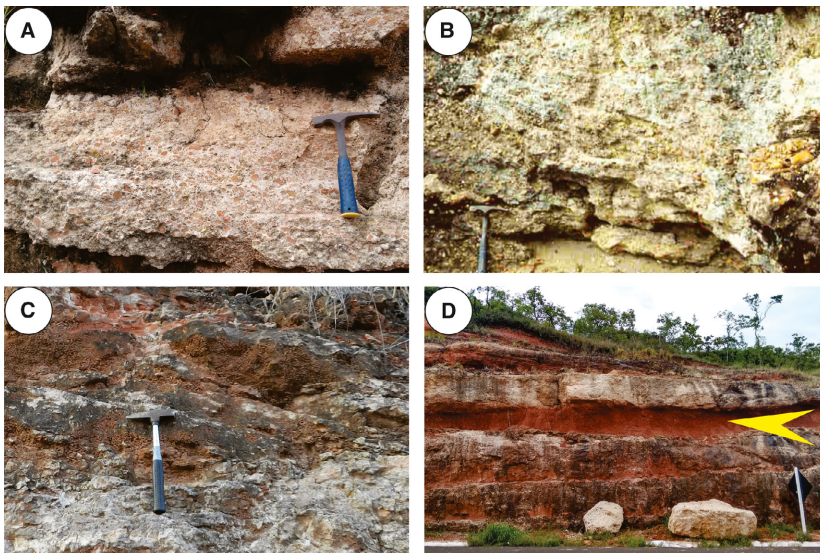


**Fig. 7.** The ephemeral ribbon channels facies association of the Bauru DFS. (A) Clast-supported conglomerate (Gm facies). (B) Trough cross-stratification and carbonate nodules in conglomerate (Gt facies). (C) Trough cross-stratification in medium to fine-grained sandstone (St facies). Hammer for scale is 40 cm long. (D) Reddish mudstone with carbonate nodules (yellow arrow). Measuring stick is 1.5 m long.

evolution occur. Based on the macromorphology and micromorphology characteristics, three palaeosol sequences are identified in this work: Uberaba, Campina Verde and Gurinhata.

*Uberaba palaeosol sequence.* Frequently associated with the braided channel belt facies association in the eastern portion of the study area, this palaeosol sequence is constituted by two palaeosol profiles interlayered with conglomerates and sandstones, and limited by erosive surfaces and compound channel elements. These profiles are composed of Bk and Ck horizons (Fig. 10) and can be classified as Aridisols and Inceptisols in comparison with modern soil taxonomy (Soil Survey Staff, 2006) (Figs 1 and 10). Because of the relationship between the facies and the palaeosols, Section 3 is used as a reference section for this part of the study area.

Profile 1 (P1, Fig. 10) is composed of the C1, C2 and C3 horizons and is massive, bioturbated and light grey (10R6/1) in colour, with thicknesses varying from 1.0 to 1.5 m. It presents an erosional top contact with fluvial conglomeratic deposits. In this profile, the C horizon presents rhizoliths associated with carbonate nodules composed of  $\text{CaCO}_3$ . Profile 2 is composed of the C1, Bk2 and Bk1 horizons with high concentrations of carbonate. This profile is 1.5 m thick (Fig. 10), and the structures are prismatic with root marks, nodules and hardpans. In the Bk horizon, micrite replaces the grains and fills primary pores. The microfabric presents a large variety of alveolar septal structures (Fig. 11A), convolute fabrics, and columnar structures composed of dark brown micrite and microsparite

laminae. Filaments and calcified roots are common as citomorphic calcite and *Microcodium* (Fig. 11B, C and D).

*Campina Verde palaeosol sequence.* This palaeosol sequence presents the most number of palaeosol profiles in the study area (Sections 4, 5, 6, 7 and 8; Fig. 1), occurring in ca 70% of the described sections. To illustrate the relationship between facies and palaeosols, stratigraphic Section 8 composed of facies and palaeosols (Campina Verde palaeosol sequence) was selected as a reference section. Ten palaeosol profiles were identified interlayered with facies (sandstones and conglomerates), and limited by erosive surfaces and compound major architectural elements (channels, overbank and aeolian deposits). These palaeosols consist of Bk, Bt, Btk, C and Ck horizons (Fig. 12) and are classified as Aridisols, Alfisols, Inceptisols and Entisols in comparison with modern soil taxonomy (Soil Survey Staff, 2006).

*Palaeosols with Btk and Bt horizons (Aridisols/Alfisols).* The palaeosols with Btk can reach up to 1.8 m thick each, or they can constitute profiles with different well-developed palaeosols rich in carbonate (Fig. 13A). The carbonate Btk horizons are usually characterized by high quantities of white  $\text{CaCO}_3$  nodules (N/8) that can account for more than 50% of the horizon. The nodules are irregular in shape, amygdaloidal and sometimes rounded, and they vary from 0.5 to 5.0 cm in size (Fig. 13B). Concretions and hardpan zones are common and are classified as pisolithic, laminar and chalky (*sensu* Alonso-Zarza, 2003; Alonso-Zarza & Wright, 2010). These

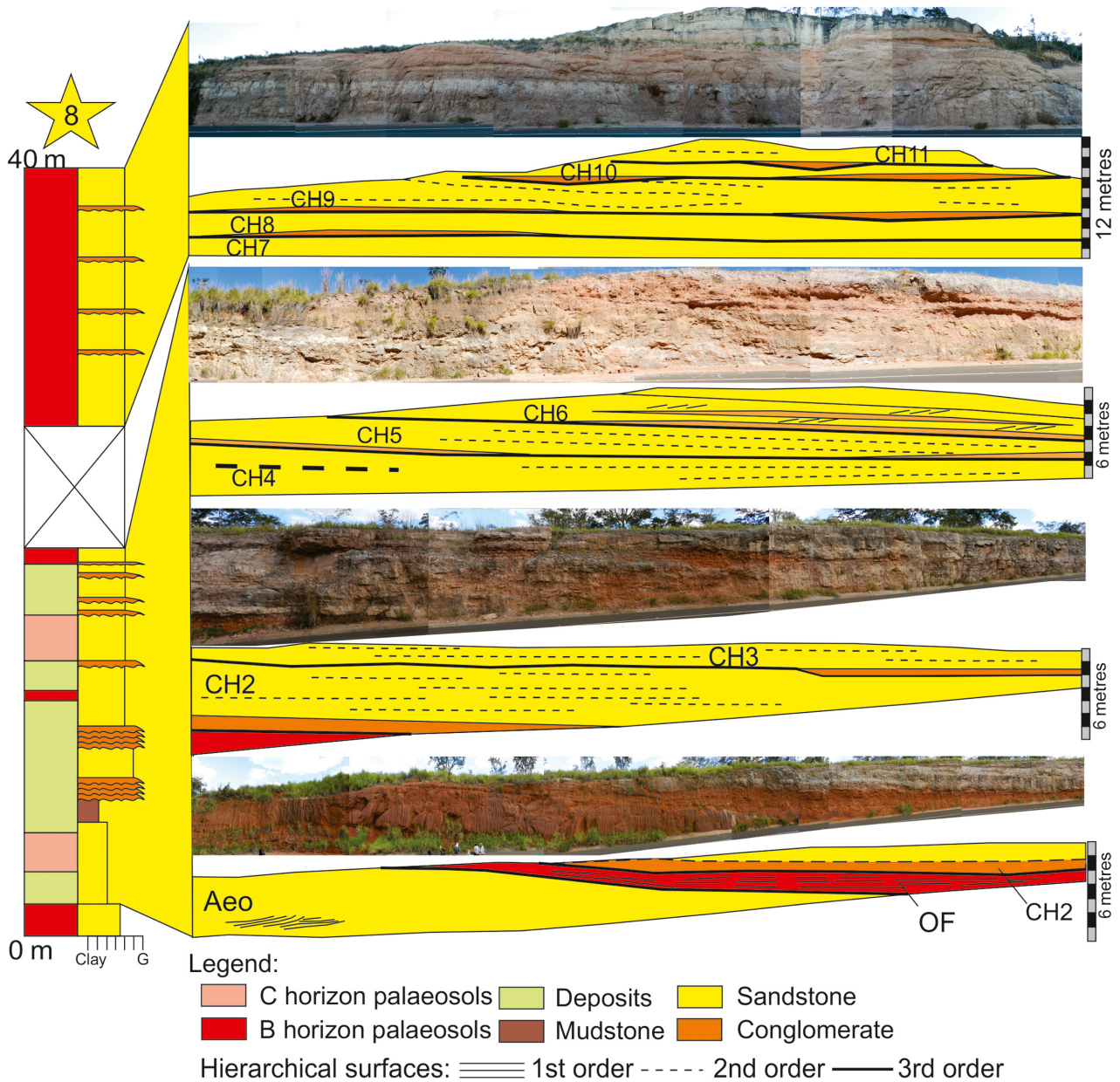


**Fig. 8.** Stratigraphic Section 8 and the architectural elements of the presenting facies and palaeosol stacking (Campina Verde reference section).

palaeosols are predominantly light red (10R6/6) and white (10YR8/1) in colour with sandy textures, and they present blocky or prismatic structures varying from 5 to 15 cm (Fig. 13C). Root marks (rhizoliths) occur in all of the profiles, with dimensions from 20 to 100 cm (Fig. 13D).

The common sequence of these palaeosols is Bt–C or Btk–C. Despite the occurrence of root marks near the tops of the palaeosols, no organic matter is preserved to characterize the A horizons. Most of the contacts between profiles are abrupt and commonly are obliterated by

carbonate cement. The Btk horizons are characterized by coatings of clay and micritic calcite with cristallitic b-fabric, calcium carbonate layers surrounding the grains of the coarse fraction, and pendant and subhorizontal microlaminar structures (Fig. 13E). Alveolar septal structures are composed of laminar interlaced micrite that fills the pores and covers the coarse grains. Clay minerals and oxides give brown tones to the carbonate (Fig. 13F).

The palaeosols with Bt horizons are well-developed and 1.0 to 1.8 m in thickness, pale



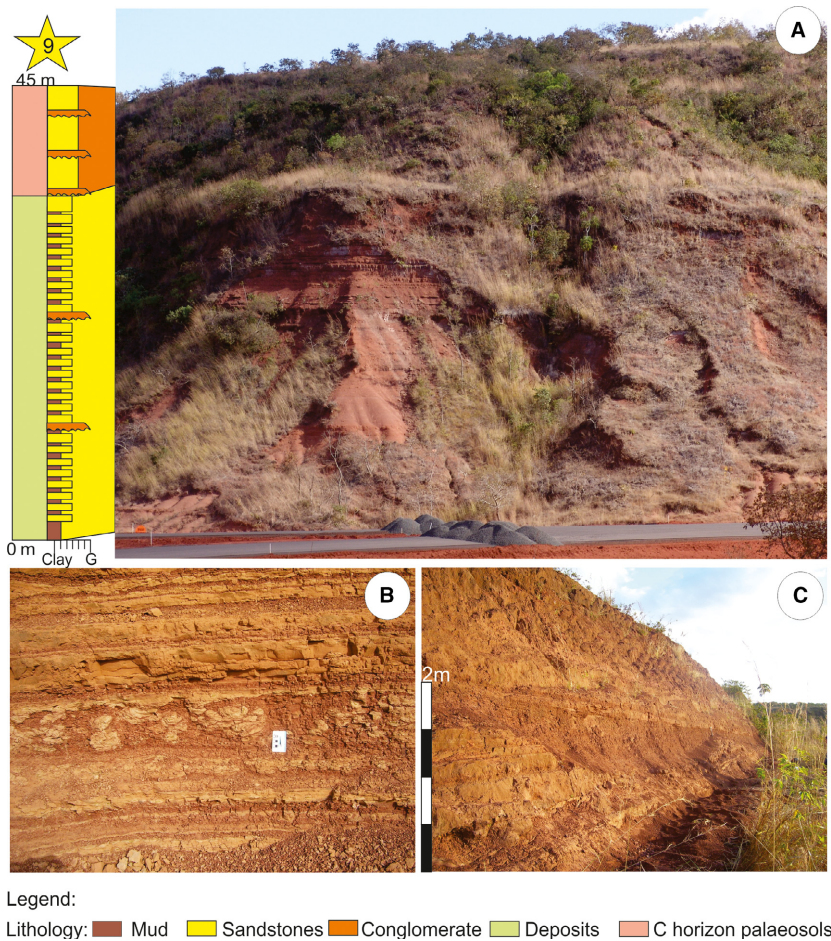


**Fig. 9.** Unconfined fluvial facies association of the Bauru DFS. (A) Panoramic view of the contacts between a muddy rhythmic succession (base), sandstones and palaeosols (top). (B) Detail of the muddy rhythmic cycles (LS element) (5 cm scale card). (C) Intraformational conglomerate cutting and filling small channels (CH element) over rhythmite deposits.

red (10R6/4) and red (10R4/8) in colour; they have small to medium block structures and clay coatings on the ped surfaces. Prismatic and block ped structures are present in the whole outcrop; however, they are more developed in the basal portions of the horizon with the presence of sparse  $\text{CaCO}_3$  nodules. Small nodules of  $\text{CaCO}_3$  (<1 cm) are associated with root marks and invertebrate traces of different types. These root marks vary from 0.3 to 40.0 cm in size, have tubular shapes and are filled with calcite (Fig. 14A). Bioturbations are filled with sand or clay minerals coming from the upper portion of the profile, with grain sizes and/or colours distinct from those of the surrounding material (Fig. 14B).

The Bt horizons contain limpid reddish illuvial clay, and whitish colours are commonly associated with the nodules and  $\text{CaCO}_3$  concentration haloes. There is up to 30% clay content in these horizons, and they are constituted by illite, montmorillonite and palygorskite (Fig. 14C) (Batezelli, 2015). The illuvial clay and carbonate occur as

coatings filling the pores and covering the grains (Fig. 14D).

*Palaeosols with Bk horizons (Aridisols).* Palaeosols with Bk horizons (two profiles) are characterized by high concentrations of calcium carbonate. The palaeosols range from 1.0 to 1.5 m thick (Fig. 15A), and the structures take the form of angular blocks (Fig. 15B), but planar structures also occur. The carbonate nodules are 3 to 5 cm in size (Fig. 15C). The nodules are coalescent in some portions of the profile, resulting in a planar appearance and forming hardpans, similar to the characteristics described in Alonso-Zarza & Wright (2010), Lintern (2015) and Zamanian *et al.* (2016). Bioturbation is common, like that occurring in the Bt and Btk horizons. Rhizoliths and invertebrate traces vary from 0.3 to 50.0 cm and are sometimes filled with poorly sorted sandy sediments cemented by  $\text{CaCO}_3$  (Fig. 15D).

In the Bk horizons, the micrite and microsparite associated with displacive and replacive fabric cementation replace grains and fill primary

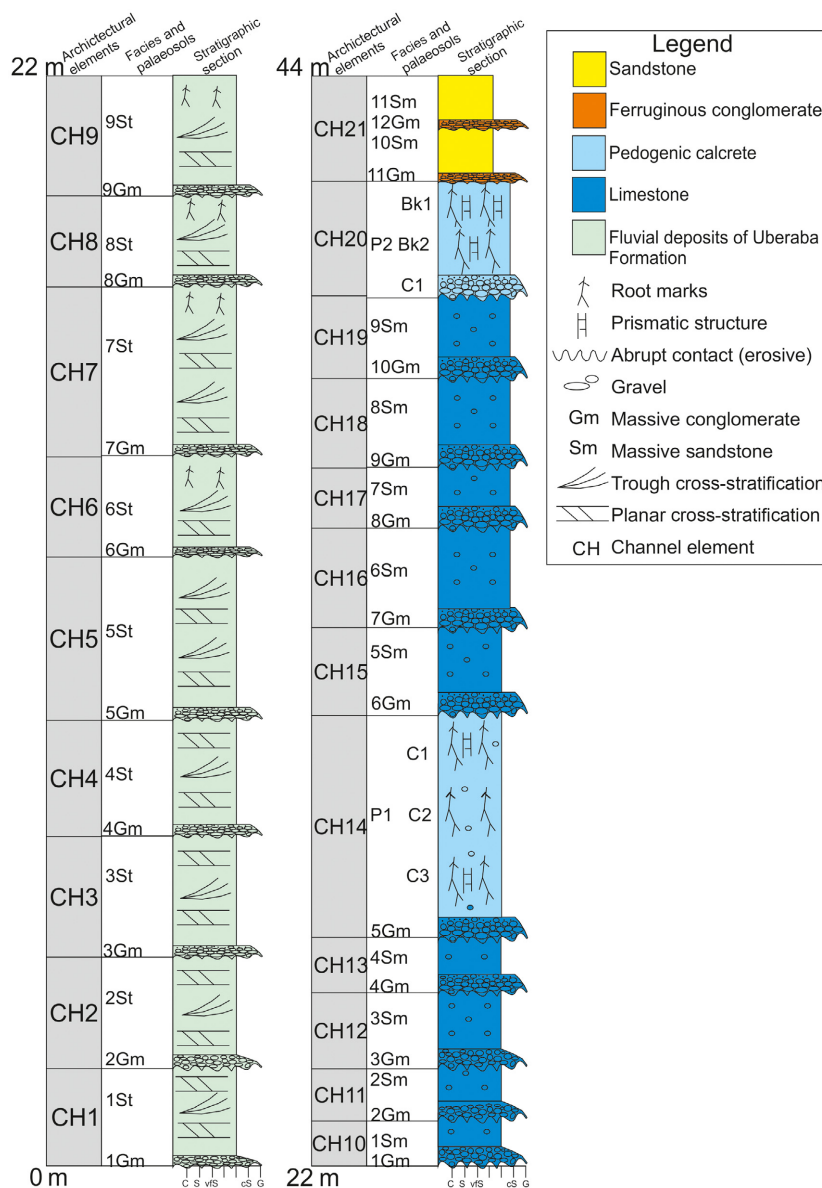


**Fig. 10.** Facies and palaeosol profiles of the Uberaba area in western Minas Gerais (Uberaba Palaeosol Sequence). Detail of Section 3 (Fig. 1) described in km 132 of the BR-050 road (from Uberaba to Uberlândia).

pores, resulting in a 'loose' arrangement in which grains 'float' in a micritic matrix (Fig. 15E). This process results in a calcite-rich groundmass with a calcitic crystalline b-fabric. Alveolar septal micritic structures also occur in these palaeosols (Fig. 15F).

*Palaeosols with C and Ck horizons (Inceptisols/Entisols).* These palaeosols comprise C and Ck horizons. They are massive and bioturbated, with thicknesses varying from 0.5 to 2.5 m, are light grey (10R7/1) and pinkish white (5YR8/2) in colour and lack a diagnostic horizon (Fig. 16A). The reference section presents

successions of stacked Ck–C, Ck or C horizons, truncated by fluvial conglomeratic deposits.

Rhizoliths are abundant and filled with calcic sandy sediments, and in the Ck horizons the rhizoliths are associated with carbonate nodules. These nodules range from 4 mm to 3 cm in diameter, and they are frequently cemented by  $\text{CaCO}_3$  and filled by medium-grained sand (Fig. 16B).

The C horizons are slightly reactive or non-reactive to HCl, and carbonate nodules are rare and sparse. This palaeosol developed under tabular bodies of sandstone with thicknesses varying from 90 cm to 1.30 m and, due to the low

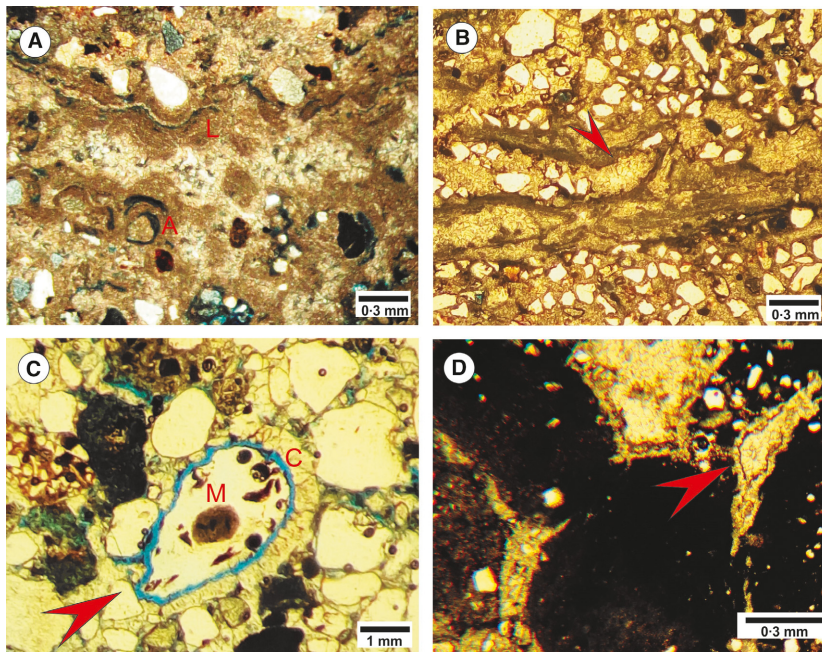


**Fig. 11.** Micromorphology of the Bk horizons. (A) Biological alveolar septal structure ('A' and 'L'). (B) Citomorphic calcite (red arrow) associated with calcified root trace (red arrow). (C) Detailed transversal view of the preserved root ('M' – medulla; 'C' – cortex) (red arrow). (D) Microcodium formed by calcified root cells (red arrow).

degree of development, some sedimentary structures are still preserved.

In the Ck horizons, the intense micritic and microsparitic cementation disturbs the sedimentary fabric, resulting in grains floating in the matrix (Fig. 16C) and, in some cases, alpha cementation (e.g. Wright, 2007), euhedral calcite crystals and dissolution features are common. Micromorphological features observed in the C horizons are less expressive. Here, the b-fabric is undifferentiated and does not present any type of orientation (Fig. 16D).

*Gurinhata palaeosol sequence.* In the western part of the study area, palaeosols occur in ca 20% of the described sections. The reference section representing the relationship between facies and palaeosols is stratigraphic Section 10 (Gurinhata palaeosol sequence – Figs 1 and 17). A succession of Ck horizons that developed over fluvial facies (sandstones and conglomerates) was identified in this section with the top limited by erosive surfaces and the compound channel elements abruptly overlying the upper portions of the laminated sand-sheet deposits (LS element). This Ck horizon succession reaches ca 15 m thick.

Individually, the Ck horizons show thicknesses ranging from 0.7 to 1.3 m. They are light red (10R6/6) and massive and have many carbonate nodules ranging in diameter from 1 mm to 5 cm. At some levels, the concentration of carbonates is so great that it forms hardpans up

to 15 cm thick and a few tens of metres in length.

Root marks and invertebrate bioturbations are common, and they are filled by sand and  $\text{CaCO}_3$ . The micromorphology analysis has identified micritic and microsparitic cementation, in addition to alpha features (e.g. Wright, 2007). The b-fabric is undifferentiated and crystalline and comprises pedoplasmated material, such as that described in the Ck horizons of the *Palaeosols with C and Ck horizons (Inceptisols/Entisols)* section.

### Bauru distributive fluvial system reconstruction and stratigraphic architecture

Regional analysis shows lateral and vertical variations in the Bauru DFS facies associations. In the maps of facies distribution, based on the percentages of sandstone and mudstone from the columnar sections and well logs (Tables 1 and 2; Fig. 18A and B), there is a decrease in the sand facies and an increase in the fines facies from east to west in the study area. Braided channel belt deposits are more common in the eastern part, while ephemeral ribbon channels and unconfined channels increase progressively from the central to the western areas (Fig. 18C). Westward of the study area, the channel deposits present decrease in size and thickness, and a gradual transition between coarse-grained active braided fluvial facies to unconfined fluvial facies is observed.

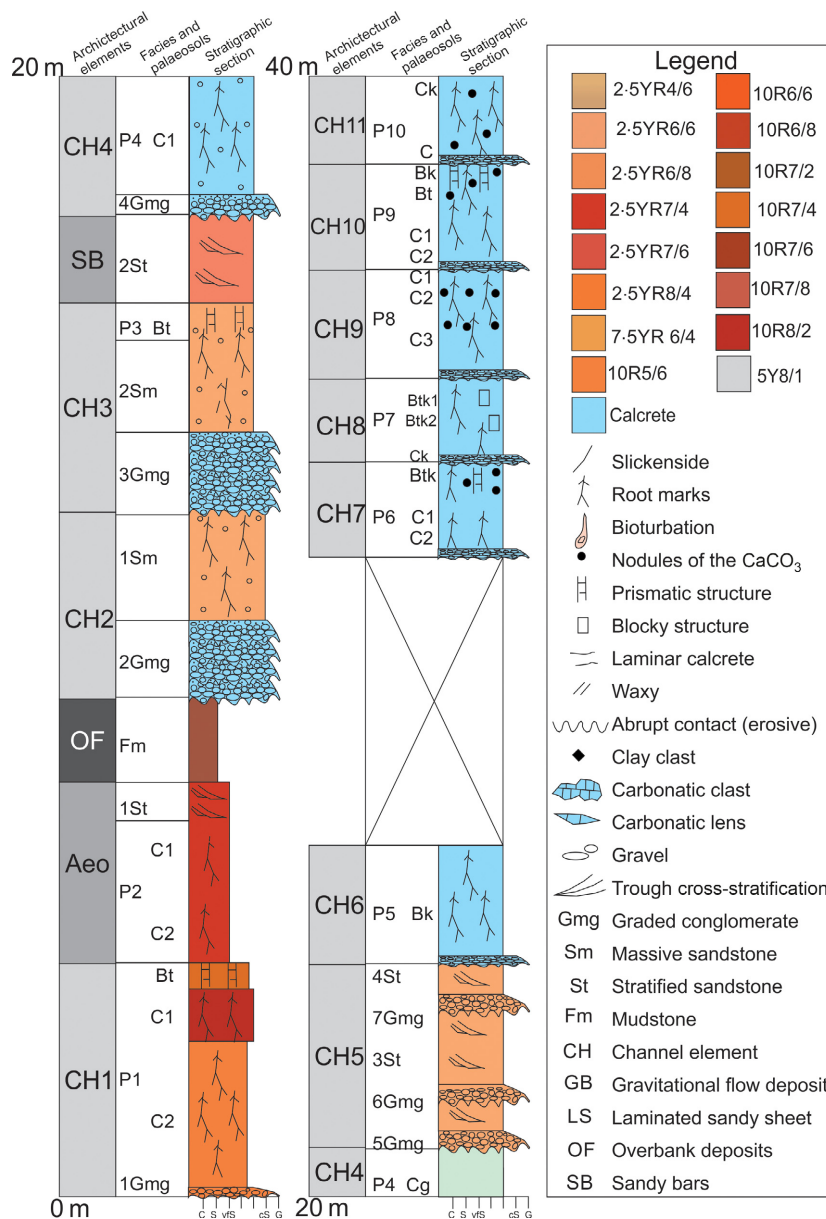


**Fig. 12.** Facies and palaeosol profiles of the Campina Verde area in the western part of Minas Gerais (Campina Verde palaeosol sequence). Detail of Section 8 (Fig. 1) described from km 153 of the BR-364 road (from Campina Verde to Gurinhatã).

The palaeocurrent data of the trough cross-bedded sandstones present high dispersion but generally indicate sedimentary transport from the east and north-east to the west and south-west. From the regional analysis, it is possible to identify a correspondence between the facies associations and the types of palaeosol profiles (Fig. 18D). This characteristic of palaeocurrents associated with the compositional maturity of the sandstones westward, as well as the distributions of facies and architectural elements, allows the division of the study area into proximal, medial and distal portions of the distributive fluvial system (DFS) with a source area in

the Alto Paranaíba Uplift (SAP), located in the east to north-east (Fig. 18D).

#### *Proximal fluvial deposition and pedogenesis*

In this domain of the study area, the most common architectural elements are amalgamated conglomeratic channels (CH element) cemented by calcium carbonate. The largest architectural elements are the channels (CH), with lateral dimensions greater than 1000 m and thicknesses of up to 70 m. Channel deposits were previously identified in this area by Alves (1995), Ribeiro (2000), Ribeiro (2001), Capilla (2002) and Batezelli (2003).

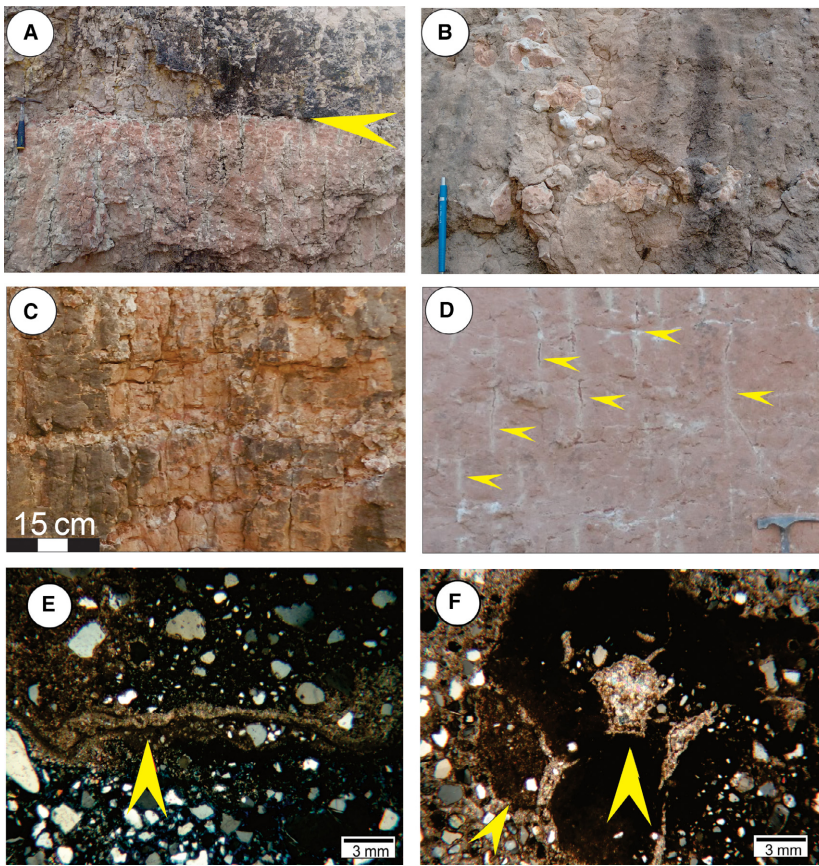


**Fig. 13.** (A) Morphological aspects of a palaeosol with Btk horizon and contact between profiles (yellow arrow). Hammer for scale is 40 cm long. (B) Nodules of CaCO<sub>3</sub>. Pencil for scale is 13 cm long. (C) Block structures in a well-developed Btk horizon. (D) Rhizoliths with carbonate in Campina Verde palaeosol sequence (hammer head is 20 cm wide). (E) Thin section of Btk horizon. Yellow arrow indicates pendants of micrite in porous space of the microstructure. (F) Glaebole of brown micrite (small yellow arrow) associated with an alveolar-septal structure. The yellow arrow indicates the micro-sparite.

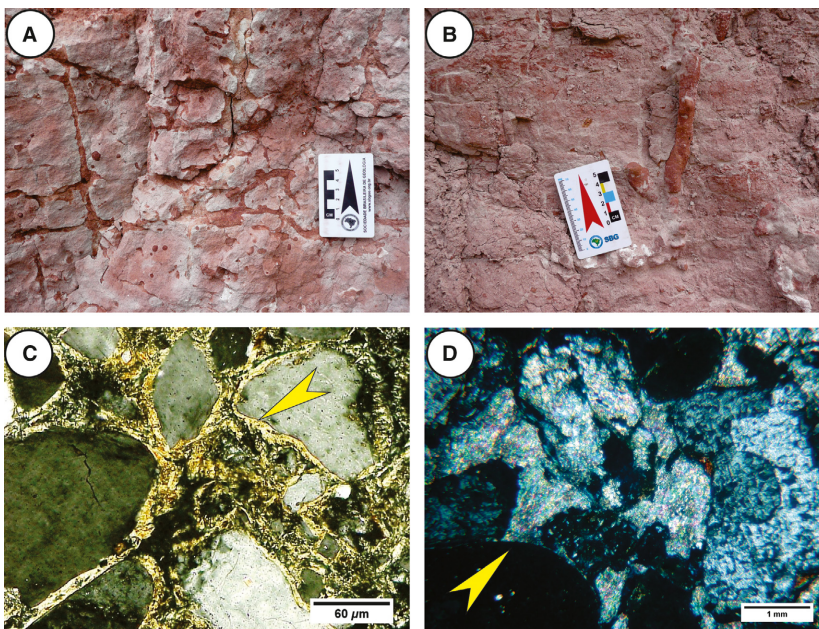


**Fig. 14.** (A) Root marks in the Bt horizon of the Campina Verde palaeosol sequence. (B) Bioturbation filled by sandy sediments – 5 cm scale card in (A) and (B). (C) Illuvial clay in Bt horizon. (D) Carbonate coating in the grains.

The vertical facies succession is characterized by thick conglomerate bodies at the base and sandy channel deposits at the top. In addition to the decrease in grain size, there is also a

decrease in the thickness of the strata, as well as an increase in textural and mineralogical maturity. In the five sections described in this area (Sections 1, 2, 3, 11 and 12 – Fig. 1), more than

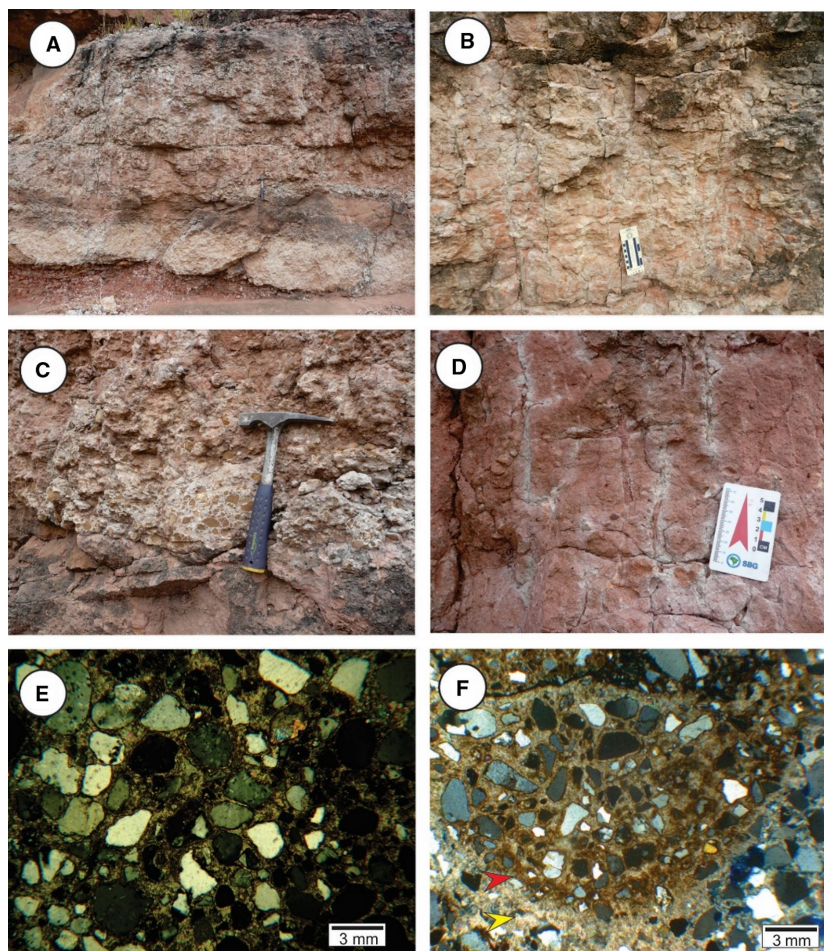


**Fig. 15.** (A) Morphological aspects of Bk horizons. Hammer for scale is 40 cm long. (B) Detail of structures in blocks (scale card is 10 cm). (C) Detail of carbonate nodules. (D) Rhizoliths filled with sand and carbonaceous material (scale card is 5 cm). (E) Micromorphological aspect of calcitic crystallitic b-fabric. (F) Micritic envelopes (red arrow) interspersed with micro-crystalline calcite (yellow arrow) associated with biological activity.

70% of the bodies constitute thick channel deposits.

Supplied by the Precambrian basement and Cretaceous magmatic rocks (Bambuí Group and Tapira alkaline-carbonatite complex), the carbonate cementation was generated by two mechanisms; groundwater dynamics and pedogenesis. In this part of the study area, the characteristics observed in lenticular carbonate sandstones and carbonate conglomerates (massive, forming layers up to 8 m thick, intense replacement of the terrigenous grains by carbonate, calcite spar and micrite-dominated alpha fabric) are similar to those of the groundwater calcretes described in Pimentel *et al.* (1996), Nash & McLaren (2003) and Wright, (2007).

Pedogenic calcretes can occur such that they are associated with the top of the fluvial deposits; however, they are found mainly in the upper portion of Section 3 (Figs 1 and 10). These palaeosol profiles present mainly C horizons (subordinate Bk) with massive and small prismatic structures and root marks and are eroded

at the top by the coarse-grained channel facies prior to deposition of the overlying channel deposits.

Citomorphic calcite occurs as sparitic crystals surrounded by calcite depletion hypocoatings, indicating the impregnation of root tissues in the carbonate soils of semi-arid areas (Jaillard *et al.*, 1991; Herrero *et al.*, 1992; Durand *et al.*, 2010). These crystals fill the porosity generated by the roots, the space of alveolar septal structures and micrite laminae in the carbonate soils, where the biological activity is high (Khormali *et al.*, 2003).

Alveolar septal structures are common in rhizogenic carbonatic horizons, associated with roots and filling the intragrain porosity. They occur in the form of irregular circular to subcircular voids and are composed of impure micrite, interpreted as resulting from biological activity, and associated with fungi biofilms (Wright, 1986; Alonso-Zarza, 1999). The voids can be filled by citomorphic calcite as a result of the root traces.

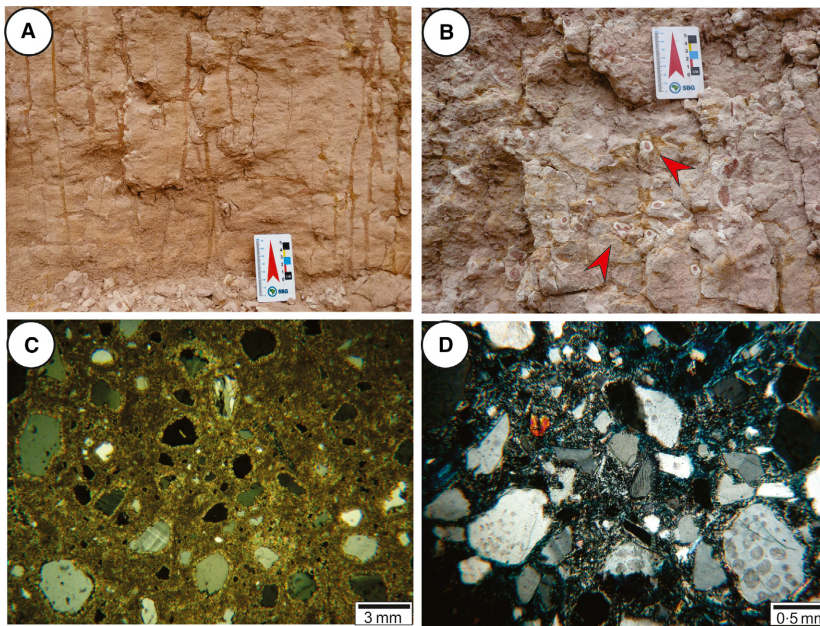


**Fig. 16.** (A) Red and grey colours of the Ck horizon. (B) Rhizoliths in Ck horizon. Arrow indicates carbonate nodules associated with root activity. Scale card in (A) and (B) is 5 cm. (C) Micro-morphological aspect of the Ck horizon. Note the intense cementation by CaCO<sub>3</sub> that disorganizes the fabric of the sandstone (floating contacts). (D) Undifferentiated b-fabric of the C horizon in response to low degree of development.

A Microcodium is an individual aggregate of calcite crystals in the calcretes (Kosir, 2004). In this work, these crystals present pyramidal and prismatic shapes distributed in radial fibres surrounding a central void (type 1 Microcodium of Plaziat & Freytet, 1978) and as several layers arranged irregularly around a central void with transverse cross-sections (type 3 Microcodium of Plaziat & Freytet, 1978). The origin of these structures is associated with the intracellular calcification of roots (Klappa, 1978, 1980; Wright *et al.*, 1995; Alonso-Zarza *et al.*, 1998; Kosir, 2004). The macromorphological and micromorphological characteristics suggest a low degree of development compared with the modern soil taxonomy of Inceptisols and eventually Aridisols (Fig. 19).

The low frequency of palaeosol occurrence in this part of the study area could be related to the high sediment supply rate and the frequent incision and shifting of channels; in addition, the high-level phreatic conditions (indicated by the intense replacement of terrigenous grains by carbonate and the presence of calcite spar and micrite-dominated alpha fabric groundwater calcretes), have not allowed pedogenesis. The constant changes in the landscape would not allow weathering for significant periods of time.

#### *Medial fluvial deposition and pedogenesis*

The medial portion is characterized by sand bars and ribbon channel deposits. The channels (element CH) include a combination of Gm, Sm and

St facies, as well as smaller-scale elements (SB and OF). Trough cross-bedded sandstones associated with conglomerates in fining-upward cycles suggest deposits in the active channels. Conglomerates occur in perennial channels in successions fining-upward with a low lateral migration rate and a gradual decrease in energy towards the top, typical of a braided river environment in the medial to distal portions of the alluvial system (Ramos & Sopena, 1983; Miall, 1996). The channels described in the study area show width/depth ratios of more than 15 : 1 and represent the ribbon channel belt (Friend, 1983; Eberth & Miall, 1991; Miall, 1996; Gibling, 2006; Currie *et al.*, 2009; Weissmann *et al.*, 2013).

In this area, palaeosols occur in more than 70% of the described sections and are characterized by argillic and carbonate horizons (Bt, Btk and Bk). Out of the 10 profiles described in Section 8, five profiles present Bt horizons, characterized by the translocation of clay from the upper horizons. The clay content in the argillic horizon is up to 20%, and illite, montmorillonite and palygorskite are the most common clay minerals in the palaeosols. Palygorskite occurs in intertwining fibrous aggregates that form nodular structures. According to Khormali *et al.* (2003), palygorskite is a magnesium aluminium silicate whose structural formula is [Mg, Al] Si<sub>8</sub> O<sub>20</sub>(OH)<sub>3</sub> (H<sub>2</sub>O) M, where M represents a mutable cation. The mineral forms under conditions of high Mg and Si concentrations, and formation water with high pH.

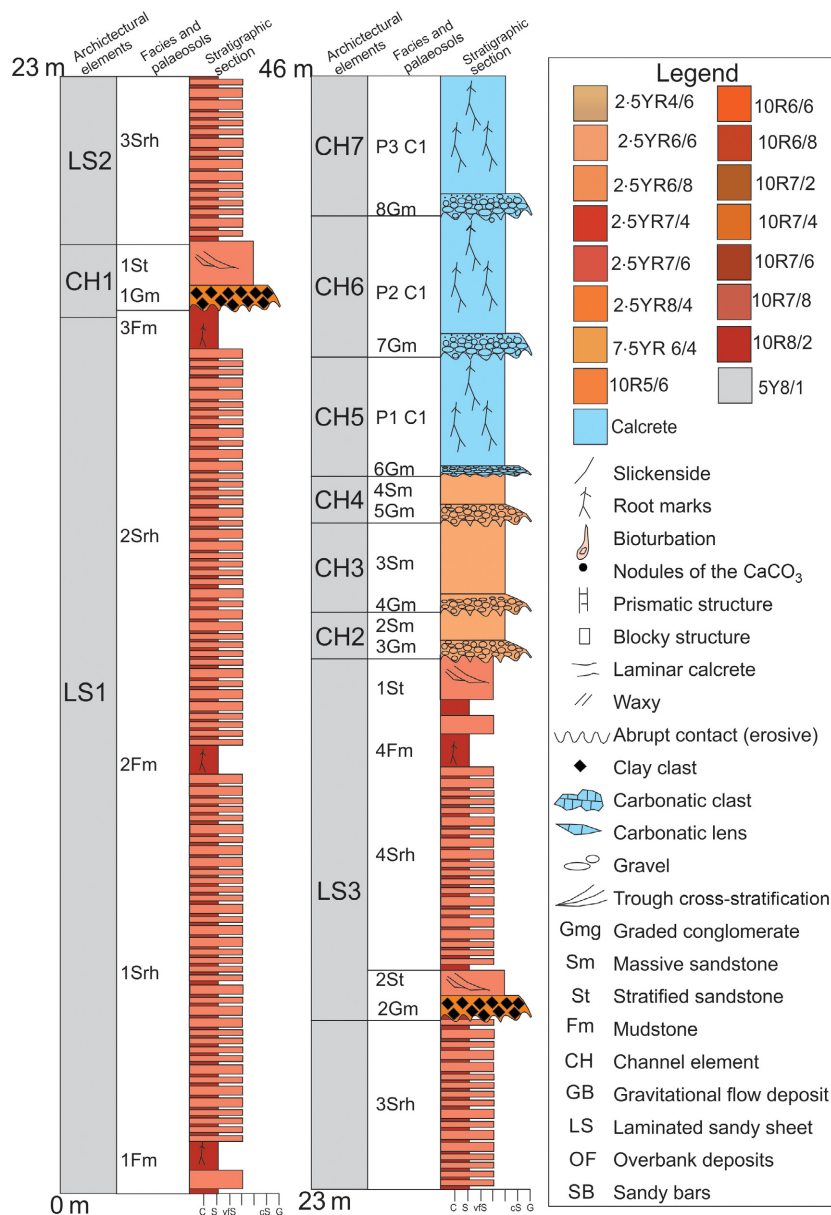


**Fig. 17.** Facies and palaeosol profiles from the Gurinhatã area in the western part of Minas Gerais (Gurinhatã palaeosol sequence). Detail of Section 9 (Fig. 1) described in km 176 of the BR-364 road (from Campina Verde to Gurinhatã).

The formation of palygorskite and carbonatic horizons has been associated with arid to semi-arid conditions (Goudie, 1983; Wright & Tucker, 1991; Abtahi & Khormali, 2001; Khormali *et al.*, 2003; Daoudi, 2004; Silva *et al.*, 2017a,b,c), usually with rainfall amounts between 500 mm and 1000 mm (Wright & Tucker, 1991). The fact that palygorskite stands out in well-developed Bt and Bk horizons is related to both its position in the landscape and good drainage.

The carbonate palaeosol profiles described in this part of the study area containing high concentrations of CaCO<sub>3</sub> consist of Ck, Bt, Bk and Btk horizons, and are classified as pisolitic, laminar, and chalky (Alonso-Zarza, 2003; Alonso-

Zarza & Wright, 2010; Pereira *et al.*, 2015; Silva *et al.*, 2015; Silva *et al.*, 2016; Nascimento *et al.*, 2017; Silva *et al.*, 2017a,b,c), indicating varying degrees of development. The thick, well-developed palaeosol profiles with Bt and Bk horizons were probably formed over hundreds or thousands of years (Birkeland, 1999), indicating stable surfaces and low sedimentation rates (Alonso-Zarza & Silva, 2002). Carbonate nodules indicate stages 4 and 5 of calcretization (*sensu* Alonso-Zarza & Wright, 2010) (Fig. 13B) and suggest periods of maximum accumulation of CaCO<sub>3</sub> related to the incision of the main drainage or climatic seasonality, as noted by Meléndez *et al.* (2011) in the Ebro Basin, Spain.



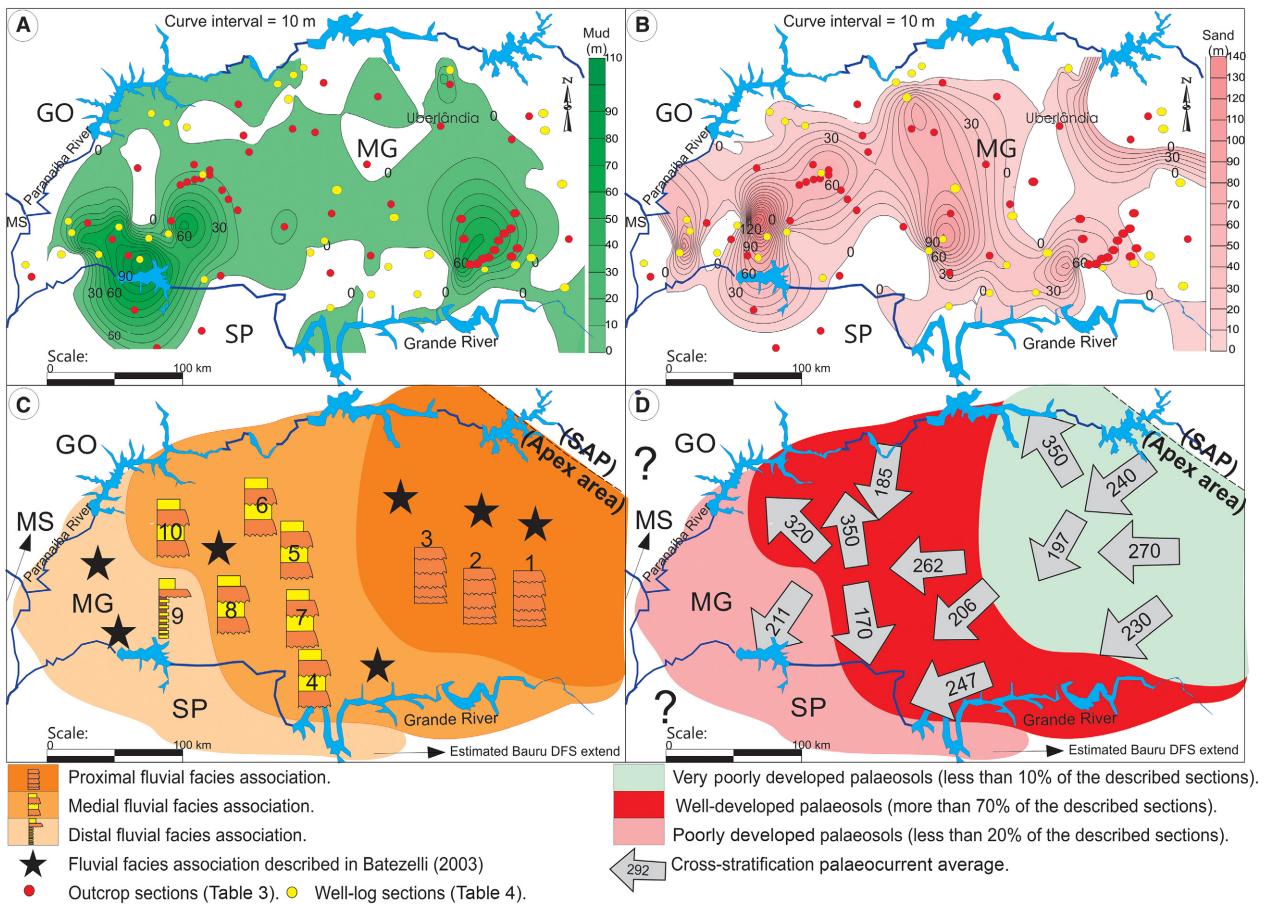


**Fig. 18.** (A) and (B) Maps of the muddy and sandy facies isopachs of the Bauru distributive fluvial system (DFS) based on outcrops and well-logs. (C) and (D) Facies association, palaeosols and palaeocurrents of the Bauru DFS in west Minas Gerais (Brazil).

In general, well-developed calcretes such as those found in the medial portions indicate low rates of sedimentation and erosion that allowed the development of thick cumulative palaeosols with platy and hardpan horizons (Fig. 13A and C). These characteristics may represent tens or even hundreds of thousands of years of development, requiring relatively stable climatic and topographic conditions, as reported in Marriott & Wright (1993), Kraus (1999) and Candy and Black (2009). McFadden & Tinsley (1985), analysing Pleistocene calcretes from California, remarked that the evolution from stage 1 to stage 2 (*sensu* Alonso-Zarza & Wright, 2010) can take up to 200 kyr in semi-arid alluvial environments. Using the U–Pb method, Candy *et al.* (2003) and Candy & Black (2009) found similar ages for the calcretes of Quaternary fluvial terraces. The long-term evolution allows the concentration of carbonate and the accumulation of illuvial clay. Therefore, the palaeosols with Bt and Btk

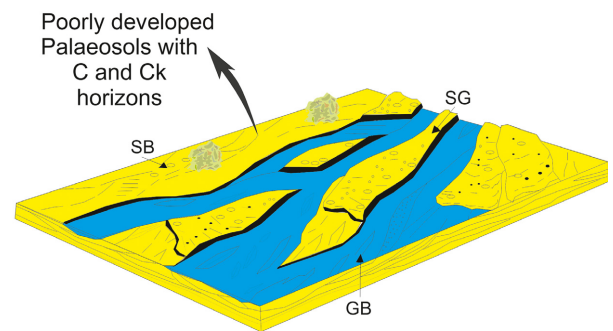


**Fig. 19.** Depositional and pedogenetic environmental model of the proximal fluvial system in the north-east Bauru Basin. Incised channels and poorly developed soils. SB = sand bars; GB = gravel bars; SG = debris flow.

horizons in the medial portion of the fluvial system in the study area suggest a stable landscape, far from areas where the fluvial channels were mobile (Wright & Marriott, 1993; Candy *et al.*,

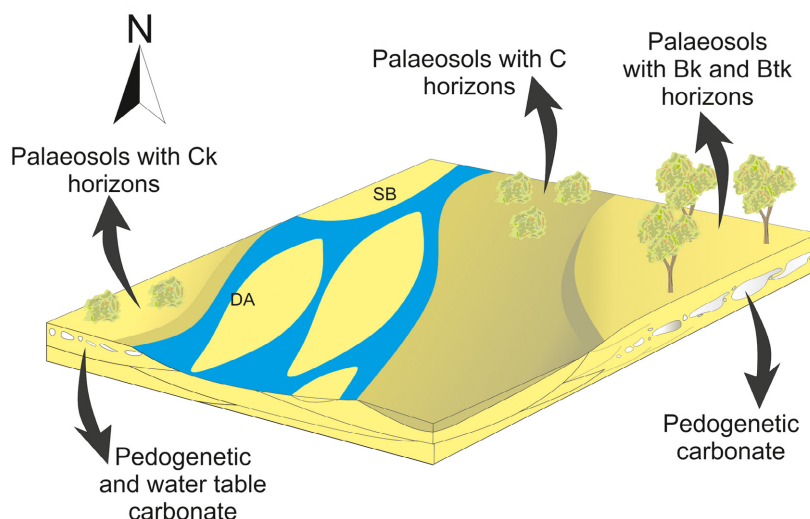


**Fig. 20.** Depositional and pedogenetic environmental model of the medial fluvial system in the north-east Bauru Basin. SB = sand bars; DA - downstream accretion.

2004; Demko *et al.*, 2004; Armenteros & Huerta, 2006; Hanneman & Wideman, 2010).

In modern alluvial systems, overbank processes and vertical accretion result in the coalescence of bars and abandoned channels, extending the plain (Miall, 1996; Nichols & Fisher, 2007; Weissmann *et al.*, 2010). In this sense, the posterior incision of the channel may result in the development of terraces or high and stable sectors in the floodplain that enable the development of mature soils with thick Bt and Btk horizons (Bown & Kraus, 1987; McCarthy *et al.*, 1999; Kraus *et al.*, 2013). Based on the facies and palaeosol characteristics, a model of the distribution of deposits and palaeosols in the medial fluvial environment in an arid to semi-arid climate is presented (Fig. 20).

#### *Distal fluvial deposition and pedogenesis*

In the distal portion, the common architectural element identified is the sheet-shaped element LS, constituting sandstone and representing deposits formed by unconfined flows or in channels with width/depth ratios exceeding 30 that were generated during flooding periods (Friend, 1983; Eberth & Miall, 1991; Miall, 1996; Gibling, 2006, Currie *et al.*, 2009). This element is associated with small channels and fine overbank deposits that formed during the decrease of energy in the alluvial plains after flooding. This element is marked at the base by a slight concave-upward third-order surface, and it abruptly overlies the ancient deposits, indicating high-energy deposition (Miall, 2010).

The elements CH and LS indicate alternation between channelized and sheet flows

(unconfined flow). Massive sandstone usually occurs in thick strata (>2 m). It is lenticular in shape and sometimes amalgamated, with dispersed clasts and ichnofossils in the form of vertical tubes and ramifications typical of roots. The association with massive conglomerate is common. The conglomerates are constituted by rounded pebbles of quartz, flint and calcrete fragments in equal proportions. In comparison with the proximal and medial portions, there is a decrease in the clast size. Massive sandstone is interpreted as a sandy bar deposit transported by low-viscosity mass flow under high-energy conditions in the medial to distal portions of the fan system (Galloway & Hobday, 1983; Ramos & Sopena, 1983; Eberth & Miall, 1991; Miall, 1996; Jones *et al.*, 2001; Batezelli, 2003; Miall & Jones, 2003; Batezelli *et al.*, 2007; Batezelli, 2015).

Based on the recognition of facies and the analysis of architectural elements, it was concluded that the deposition mechanisms were marked predominantly by high-energy laminar flows. The association of conglomerates and sandstones in channel elements indicates the activity of fluvial processes in a distal plain related to channelized or non-channelized ephemeral flows. The sandstones in the sheet-shaped LS element are similar to those in the medial to distal portions of the distributive fluvial systems, where the sediments are transported by unconfined flows or in very wide fluvial channels in the form of sand sheets (Hartley *et al.*, 2012, Weissmann *et al.*, 2013).

In the upper portion of the distal deposits, there is a succession of conglomerates Gm at the bases of thick sandstone sequences (with

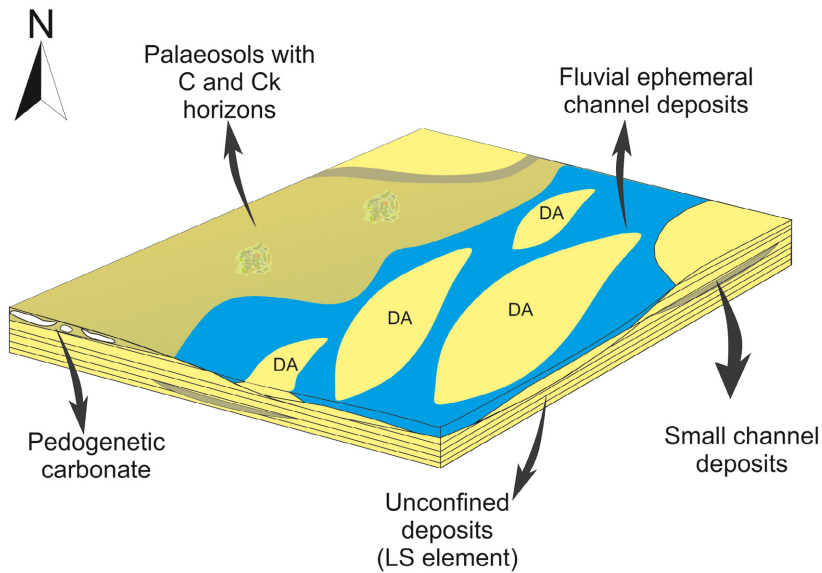


**Fig. 21.** Depositional and pedogenetic environmental model of the distal fluvial system in the north-east Bauru Basin. DA = downstream accretion.

bioturbations on top) with cyclic repetitions. At the end of each sedimentary cycle, there was a period in which the sediments were exposed to weathering and organic activity. In the following cycle, another succession of conglomerates and sandstones was deposited, overlying the previous one and generating thick strata.

The palaeosols of this area occur mainly in the upper portion of the section and are characterized by C and Ck horizons (Inceptisols and Entisols). The restricted occurrence of the palaeosols in this part of the section is similar to those described in the medial fluvial area, where ephemeral ribbon channel deposits are developed.

Buol *et al.* (2011) indicate a certain variety of conditions for the existence of these soils, such as extreme dryness, surfaces that are not regularly reached by the erosion and removal of soil portions, successive depositional events that cover the soil surface before horizons develop, and abundant materials from inert sediments (such as sandy deposits that are essentially composed of quartz). Gile (1975) states that, under arid conditions, these soils can remain lacking in B horizons for several thousands of years when the parental material is carbonate and *ca* 1 kyr when the source material is poor in carbonate, indicating that dry conditions can be responsible for keeping the pedological development low.

The palaeosol profiles described in this part of the study area containing carbonate concentrations can be classified as *transitional*, *chalky* or *nodular* horizons (*sensu* Alonso-Zarza & Wright,

2010; Pereira *et al.*, 2015; Silva *et al.*, 2015; Silva *et al.*, 2016; Nascimento *et al.*, 2017; Silva *et al.*, 2017a,b,c), presenting abundant powdery calcium and carbonatic nodules. In the palaeosols described in this part of the study area, carbonate precipitation occurred in association with roots (Fig. 16B), forming rhizoliths and increasing the CaCO<sub>3</sub> cementation.

Soil carbonate accumulation rates vary over time and between localities in response to geographic, geological and climatic controls (Machette, 1985). Studying the Roswell–Carlsbad area in the USA, Machette (1985) identified a rate of accumulation of pedogenic carbonate of 0.5 g cm<sup>-1</sup> kyr<sup>-1</sup>, in an area with an annual precipitation of *ca* 330 to 355 mm. In this way, calcrete profiles require tens of thousands of years for their formation (Wright, 2007; Alonso-Zarza & Wright, 2010; Gocke *et al.*, 2012; Silva *et al.*, 2016).

The stage 2 carbonatic palaeosols are formed near channels or valleys (Nash & Smith, 1998), which are areas of stability in the landscape, making possible the accumulation of pedogenic carbonate and generating alpha-type cementation (e.g. Wright, 2007). This characteristic indicates the strong influence of the water table. The well-developed sparite calcite crystals indicate long-term formation with a constant supply of CaCO<sub>3</sub>-rich water (Durand *et al.*, 2010), different from the eluvial/illuvial precipitation ‘per descensum’ (e.g. Goudie, 1983). All of the depositional and palaeopedological characteristics allow development of the environmental model shown in Fig. 21.

### Stratigraphic architecture

Three east–west stratigraphic sections cross-cutting the entire study area were elaborated (Fig. 22A to C). The base of the amalgamated channel belt facies association is characterized by a regional erosive surface and was used as the stratigraphic marker. Although the chronological data indicate no time hiatus, this regional surface marks upward changes in the facies associations.

In the eastern study area, amalgamated channel belt deposits are very thick (up to 70 m) and overlie the Early Cretaceous basalts of the Serra Geral Formation (Fig. 2). The east–west trending sections (Fig. 22A to C) show asymmetry, with a gradual decrease in the thickness of the amalgamated channel belt, and increases in the ephemeral ribbon channel and unconfined channel facies associations westward.

The columnar sections of the central study area show a vertical facies succession starting with the sandy ephemeral ribbon channel association overlapped by amalgamated channel belt deposits. The thickness of the ephemeral ribbon channel deposits varies from 3 m at point 8 (Campina Verde) to 45 m at point 9 (Gurinhata). In this portion, well-drained palaeosols are very common, but they become less frequent and more poorly drained moving towards the east and west.

In the western study area, the unconfined channels facies association abruptly overlies the Serra Geral Formation basalts. At the top of all of the sections, an increase in the amalgamated channel belt facies association was identified. All changes identified in the stratigraphic sections are in accordance with the maps of facies in Fig. 18A to C, indicating that progradational stacking of the facies started with the distal facies association at the base followed by the medial and proximal facies associations.

## DISCUSSION

### Tectonic and progradational fluvial system evolution in the Bauru Basin

Facies and palaeosol analyses performed in the north-eastern Bauru Basin have identified marked changes in the fluvial characteristics from the east to the west of the study area: radial channel patterns, a decrease in channel size, an increase in floodplain deposits, a decrease in grain size, changes from

amalgamated channel deposits to smaller fixed channels, and changes in palaeosol distributions. All characteristics are consistent with the distributive fluvial system (DFS) model proposed by Hartley *et al.* (2010), Weissmann *et al.* (2010), Weissmann *et al.* (2013), Owen *et al.* (2015) and Owen *et al.* (2017).

Sandy and gravelly channel deposits in the eastern/north-eastern parts of the study area suggest active confined flows in the proximal zones of the braided channel belt. The periodic incision of the proximal part was related to increases in the water flow and sediment supply. Because of the decrease in water basinward, the fluvial system became ephemeral, characterized by amalgamated ribbon channels, overbank deposits and palaeosols. In the distal part of the study area, small channels, unconfined fluvial sandy sheets and playa lake deposits dominated the palaeoenvironment, generating a coarsening-upward succession of facies.

These characteristics indicate a downstream decrease in energy, which is attributed to channel bifurcation, infiltration, evapotranspiration and the deceleration of flow as the system radiated outward from the apex (Kelly & Olsen 1993; Nichols & Fisher 2007; Weissmann *et al.* 2010; Hartley *et al.* 2010; Davidson *et al.* 2013). In recent years, different studies have described progradational fluvial systems to define the stratigraphic signatures in continental basins (e.g. Currie, 1998; Cain & Mountney, 2009; Trendell *et al.*, 2013 Weissmann *et al.*, 2013; Owen *et al.*, 2015; Owen *et al.*, 2017).

Owen *et al.* (2015, 2017) have tested the conceptual model proposed by Weissmann *et al.* (2013) via a quantitative study of the vertical trend in the prograding Salt Wash DFS. In this study, the authors determined the key controlling mechanisms responsible for progradation, retrogradation or aggradation, including changes in source area, basin and climate. Vertical sections in the Salt Wash DFS have an assigned facies domain based on the grain sizes, the architecture of the deposits and the sandstone percentages.

Based on this approach, the study conducted in the north-east Bauru Basin identified evidence of progradation in the Bauru DFS. From the stratigraphic analyses, there is much evidence to support the interpretation that the Bauru DFS prograded from east to west in the study area. The lateral changes in facies associations, coupled with a general increase in the channel belt upward in the distal area,

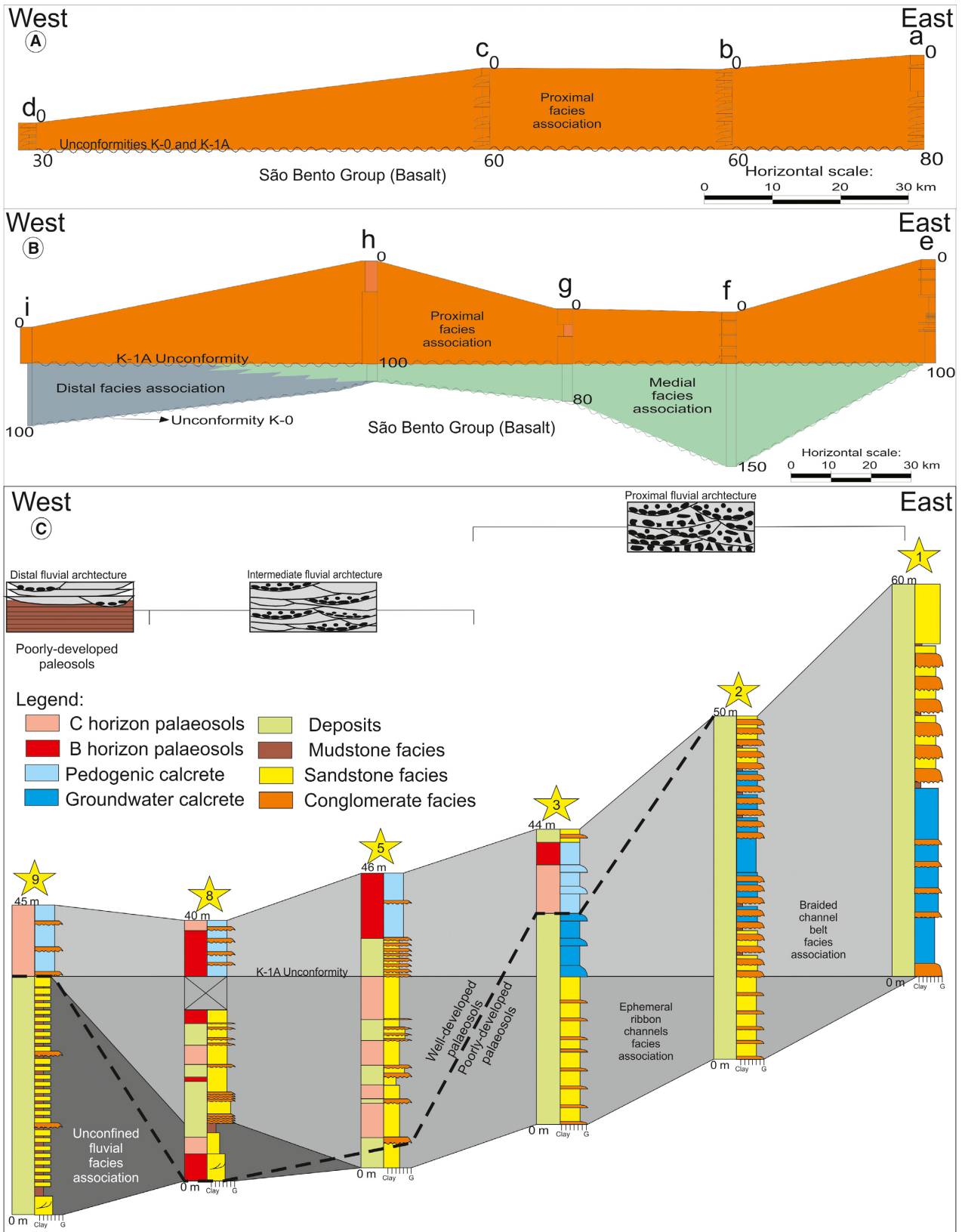


**Fig. 22.** Stratigraphic cross-sections showing the fluvial facies and palaeosol architecture in western Minas Gerais. (A) and (B) Stratigraphic sections based on the well-logs. (C) Detailed stratigraphic distribution of the facies and palaeosols based on the outcrops correlation.

generated a basin-scale stratigraphic marker (K-1A unconformity) and can be considered to be the main evidence of progradation.

In a continental system, the tectonic plates and climate are the main control agents for progradation, aggradation and retrogradation. Identifying the influences of tectonics and climate in the evolution of thin sequences is difficult; however, because autogenic factors can produce features similar to those generated by progradation or retrogradation (for example, lobe switching, avulsions and local changes in topography; Cecil, 2003; Miall, 2010; Cecil, 2013; Owen *et al.*, 2015).

In the Bauru Basin, the regional K-1A unconformity (Batezelli, 2015; Fig. 22) at the base of the braided channel belt deposits is the strongest evidence of the allogenic influence on the progradation of the fluvial system. The stratigraphic sections of Fig. 22 present, in addition to the stratigraphic marker, an increase in thickness of the braided channel belts deposits upward from east to west.

The changes in the vertical successions provide insight into the tectonic evolution of the basin, allowing an understanding of the relationship between accommodation space (A) and sediment supply (S). Substantial long-term change is needed to prograde or retrograde facies under the influence of the allocyclic scale (Owen *et al.*, 2015). In the Bauru Basin, this change was associated with the latest tectonic manifestation of the Alto Paranaíba Uplift (SAP) in the north/north-east during the Maastrichtian (Fig. 2; Batezelli, 2015). The uplift in the eastern study area generated a significant increase in sediment supply, which was responsible for the negative A/S ratio in the basin.

Tectonic processes are important in creating the stratigraphic framework for the Bauru deposition by creating a source area and space for the system to accumulate. Variable uplift rates, mainly temporally, were responsible for the architecture of the Bauru fluvial system, which could explain the vertical trends observed in the sections and the regeneration of regional stratigraphic data at the base of the braided channel belt deposits.

With the latest magmatic manifestation of the SAP, thermal uplift has renewed the Bauru Basin source area, increasing the sediment supply and propagation of the apex basinward. Sedimentation rates and palaeosol development are interpreted to be important in the stratigraphic patterns observed from east to west in the Bauru DFS.

Provenance studies performed in the study area since 1998 (e.g. Fernandes, 1998; Batezelli, 2003; Batezelli *et al.*, 2005; Batezelli *et al.*, 2007; Batezelli, 2010; Batezelli, 2015) indicate substantial changes in mineralogical composition within the Bauru Group. In accordance with these studies, the field observations and petrographic analyses herein of more than 50 samples of the sandstones and palaeosols indicate increases in Precambrian basement rock fragments from the bases to the tops of the columnar sections. In contrast, there is a progressive decrease in fragments of the younger sequences (Cretaceous volcanic rocks, Phanerozoic and supracrustal sequences), supporting the interpretation of the continuous exhumation of the basement during the Late Cretaceous in the east to north-east parts of the Bauru Basin in the Alto Paranaíba Uplift area. Although there is no quantitative analysis, the overall extent of progradation can be inferred as far west as the Minas Gerais–Goiás border and as far south as São Paulo–Minas Gerais border.

### Climatic considerations

Climate is the primary allogenic control on the sediment flow in sedimentary basins, affecting geochemical and physical processes over time (Cecil, 1990, 2003) and, consequently, it is one of the main controls in soil development. In the semi-arid Bauru DFS, the climate was one of the most important factors in the soil evolution (Goudie, 1983; Alonso-Zarza, 2003), controlling the degree of palaeosol maturity.

During the Maastrichtian, the climate was warm and arid because of the global greenhouse effect. From north to south, dune fields developed in the desert environments of the Brazilian territory, covering wide areas in the Sanfranciscana and Parecis basins (Batezelli, 2015; Batezelli & Ladeira, 2016).

Through the study of facies and palaeosols, it is possible to interpret that the climate was arid to semi-arid, specifically for the upper portion of the Bauru DFS, where Cambisols, Aridisols, Entisols and Alfisols, all of them carbonate-rich (calcretes), were identified. The braided channel river deposits and the Aridisols with Bk and Btk horizons are indicative of a semi-arid climate with a range of precipitation between 400 mm and 600 mm (Goudie, 1983). By means of palaeo-precipitation calculations, Pereira *et al.* (2015) have estimated precipitation rates between 240 mm and 400 mm (mean annual

precipitation) for the upper portion of the Bauru Group, which is consistent with the annual precipitation range for the development of calcretes according to Goudie (1983). The clay minerals illite, montmorillonite and palygorskite indicate high Mg and Si concentrations commonly found in arid to semi-arid environments with rainfall amounts between 500 mm and 1000 mm (Goudie, 1983; Wright & Tucker, 1991; Abtahi & Khormali, 2001; Khormali *et al.*, 2003; Daoudi, 2004).

Several authors have identified palygorskite in samples of the Bauru Group, suggesting their occurrence in an arid to semi-arid climate (Lepesch *et al.*, 1977; Suguio & Barcelos, 1983; Ribeiro, 2001; Barison, 2003; Fernandes, 2010; Batezelli, 2015; Silva *et al.*, 2017c). Silva *et al.* (2017c) present quantitative studies to understand the processes responsible for the changes in the percentages of palygorskite, correlating them to palaeoenvironmental changes. The results indicate that authigenic palygorskite associated with calcite and smectite formed by pedogenic processes in a warm and dry climate, with episodes of higher precipitation, humidity, leaching and desilication.

The abundance of calcretes in the study area records environments with a semi-arid palaeoclimate because calcretes are rare in arid or humid climates and develop fully in semi-arid climates (Fedoroff & Courty, 1989). Modern calcretes are common in semi-arid climate environments (Klappa, 1983; Tanner, 2010). Another factor that endorses this thesis is the lack of gley horizons associated with calcretes. Generally, calcretes from humid climates are associated with horizons of reducing environments because their position is in relief (Alonso-Zarza, 2003; Silva *et al.*, 2017b,c).

While most of the calcretes found in the proximal DFS present the features of groundwater genesis, macromorphological characteristics lead to the interpretation that the medial DFS calcretes are pedogenic because the profiles show most of the features inherent to calcretization pedological processes (Pimentel *et al.*, 1996; Alonso-Zarza, 2003; Wright, 2007; Silva *et al.*, 2017a). Calcic horizons (Bkm, Btkm and Bt), ped structures (blocky, prismatic and laminar) and the abundance and diversity of calcretes (laminar, powdery, nodular and hard crust) analysed in the medial DFS are typical macrofeatures of semi-arid climate soils (Birkeland, 1999; Retallack, 2001; Wright, 2007; Silva *et al.*, 2017b,c) and are not found together in arid environments

or systems. Micromorphological features such as calcium depletion, calcite pendants, coatings and hypocoatings, favourable palygorskite authigenesis under conditions of pH <8.5 in the pedogenic environment, cytomorphic calcite, microcodium, sparitic and micritic calcite are characteristics indicative of a semi-arid climate with seasonal variations (Klappa, 1983; Colson *et al.*, 1998; Chen & Eggleton, 2002; Durand *et al.*, 2010; Galán & Pozo, 2011; Silva *et al.*, 2017b,c). Although the mineralogy reveals the general conditions of a semi-arid climate during the palaeosol genesis, mainly in the upper unit of the Bauru Group (Marília Formation), local and regional variations are also identified, suggesting climatic cyclicity or changes in the hydrology of the Bauru Basin during the Maastriichtian (Silva *et al.*, 2017b,c).

For soils developed in alluvial plains with no carbonate cementation, such as the palaeosols of the distal portions of the Bauru DFS, the humidity as a function of the topography and the proximity to the water table makes them more dependent on the local conditions than on the atmospheric factors (Retallack, 2001). In this way, the well-developed Alfisols in semi-arid environments may indicate landscape stability and temporal hiatus, and not necessarily increased water availability caused by climatic changes (Buol *et al.*, 2011).

## CONCLUSIONS

The Bauru Group is a record of a distributive fluvial system developed during the Campanian–Maastriichtian in the Bauru Basin in southern South America. Facies analysis and palaeosol characterization of this unit in the north-eastern portion of the Bauru Basin allowed the reconstruction of the Bauru distributive fluvial system, delimiting different fluvial patterns along the longitudinal profile.

The proximal Bauru distributive fluvial system (DFS) is characterized by a braided channel belt forming a succession of deposits with thicknesses of up to 30 m. In this area, facies and the near-absence of palaeosols (Aridisols and Inceptisols) indicate high depositional rates and shifting channels. The greater declivity of the slope in this area was responsible for the high energy of the fluvial systems, promoting changes in the landscape (erosion and deposition). This lack of stability in the landscape, associated with a high level of the water table (evidenced by

groundwater calcretes), did not allow the development of thick palaeosol profiles.

In addition to the lateral variation in facies, the stratigraphic architecture varies from east to west in the system. In the most proximal sections studied (Sections 1, 2, 3, 11 and 12 – Fig. 1), the outcrops are composed of kilometres of connecting channel deposits with a high degree of amalgamation. Floodplain deposits and palaeosols are almost absent in this part of the area, suggesting a constant reworking of the sediment associated with a high degree of channel shifting.

The medial Bauru DFS is characterized by ephemeral channels, aeolian deposits and the frequent occurrence of palaeosols (Aridisols, Alfisols, Inceptisols and Entisols). Although the surface hydrology of this area was characterized by eventual floods, there was available water in the environment responsible for the developing vegetation. The well-drained condition of the exposed deposits (parent material) allowed the genesis of thick palaeosol profiles with carbonate and argillic horizons (Bk, Btk and Bt). The frequency and distribution of palaeosols in this area suggest long periods of exposure for deposits in a low-declivity landscape.

In the medial portion of the Bauru DFS, channel sandstone bodies are also amalgamated, but there is a decrease in the thickness of the conglomerates and sandstones and an increase in floodplain deposits. Channel complexes are smaller when compared with those described in the proximal area, probably because of a decrease in connectivity between the sandstone bodies. In this portion, well-drained palaeosols are present in more than 70% of the sections, indicating long periods with no sedimentation.

In the distal Bauru DFS, the fluvial system interacted with a playa lake system. The deposits are represented by muddy sandstones, mudstones and intra-formational conglomerates typical of playa lakes and ephemeral fluvial deposits. The interaction with unconfined fluvial deposits occurs in the tops of the sections in this area. The palaeosols are absent in the playa lake deposits; however, in the fluvial deposits near the tops, palaeosols are frequent (Aridisols and Inceptisols). Poorly drained palaeosols are the most common palaeosol of the low-declivity relief associated with a high water table.

The changes in deposition and pedogenesis were produced by tectonic forces and climate.

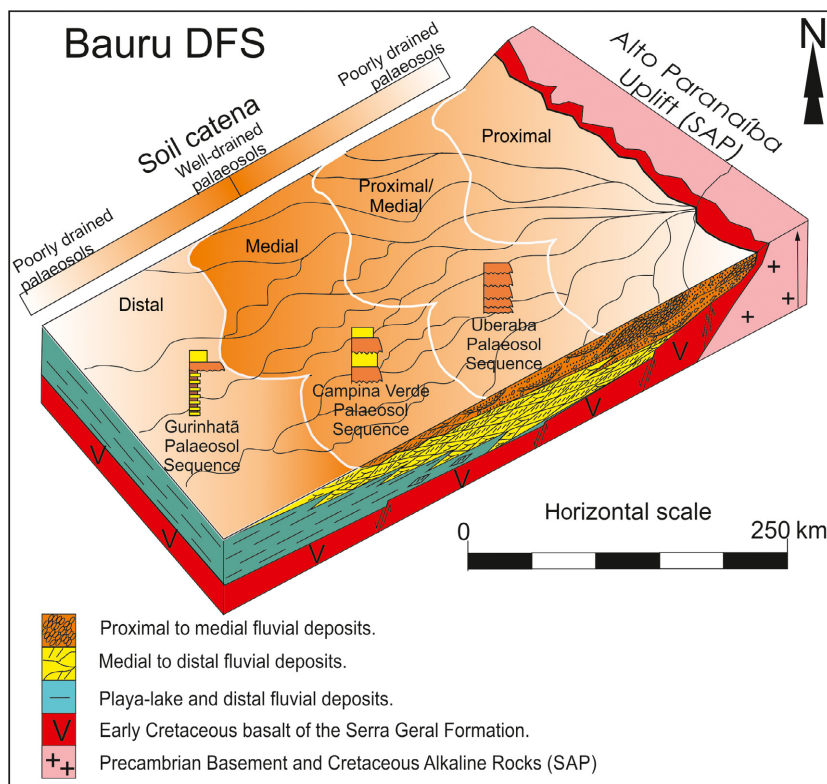


**Fig. 23.** Bauru distributive fluvial system model showing facies and palaeosol distribution in the different areas.



From east to west, the sedimentary succession records a gradual decrease in grain size, a decrease in channel width, a decrease in the lateral and vertical connectivity of channel deposits and an increase in overbank deposits, typically found in progradational distributive fluvial systems.

The increase in fine deposits, the maturity of the sandstones and the palaeocurrent dispersion basinward in the west are indicative of the progradational evolution of the Bauru DFS, with a source area in the Alto Paranaíba Uplift (SAP). The uplift in the north and north-east parts of the Bauru Basin was responsible for the increase in sediment supply, promoting the progradation of the fluvial system to the south and south-west (Fig. 23).

The palaeosol profiles interbedded with fluvial deposits suggest that evolution occurred in cycles that lasted at least tens to hundreds of thousands of years. The calcretes described at the top of the Bauru Group are responsible for the landscape, sustaining a tabular-shaped topography in all study areas. These calcretes record the last events of sedimentation and pedogenesis occurring during the Maastrichtian in the Bauru Basin.

The palaeosol distributions in the Bauru DFS record local and regional variations in depositional environment, soil drainage and geomorphology. These contemporaneous changes in palaeosol profiles caused by the position in the landscape can represent an example of a soil catena (Steila, 1976; Tabor et al., 2006).

## ACKNOWLEDGEMENTS

The authors wish to thank the São Paulo Research Foundation (FAPESP) for supporting and funding Project FAPESP 2015/17632-5: Sedimentation and pedogenesis of the Upper Cretaceous of the Bauru, Sanfranciscana, Parecis and Neuquen basins. Thanks to CNPq for the productivity grants (processes 301200/2017-3 and 308629/2015-9). Thanks to Adrian Hartley, Raul De la Horra and Ricardo Perobelli Borba for their criticisms and suggestions.

## REFERENCES

- Abtahi, A. and Khormali, F. (2001) Genesis and morphological characteristics of Mollisols formed in a catena under water table influence in southern Iran. *Commun. Soil Sci. Plant Anal.*, **32**, 643–658.
- Alonso-Zarza, A.M. (1999) Initial stages of laminar calcrete formation by roots: examples from the Neogene of central Spain. *Sed. Geol.*, **126**, 177–191.
- Alonso-Zarza, A.M. (2003) Palaeoenvironmental significance of palustrine carbonates and calcretes in the geological record. *Earth-Sci. Rev.*, **60**, 261–298.
- Alonso-Zarza, A.M., Sanz, M.E., Calvo, J.P. and Estevez, P. (1998) Calcified root cells in Miocene pedogenic carbonates of the Madrid Basin: evidence for the origin of *Microcodium* b. *Sed. Geol.*, **116**, 81e97.
- Alonso-Zarza, A.M. and Wright, V.P. (2010) Calcretes. In: *Carbonates in Continental Settings: Geochemistry, Diagenesis and Applications* (Eds A.M. Alonso-Zarza and L.H. Tanner), *Develop. Sedimentol.*, **62**, pp. 177–224. Elsevier, Amsterdam, the Netherlands.
- Alonso-Zarza, A.M. and Silva, P.G. (2002) Quaternary laminar calcretes with bee nests: evidences of small scale climatic fluctuations, Eastern Canary Islands, Spain. *Palaeogeogr. Palaeoclimatol. Palaeoecol.*, **178**, 119–135.
- Alves, J.M.P. (1995) Petrologia e Diagênese do Membro Ponte Alta, Formação Marília, Cretáceo da Bacia do Paraná, na Região do Triângulo Mineiro. Ouro Preto (MG), 102 pp. (Master Science Thesis, UFOP).
- Amaral, G., Bushee, J., Cordani, U.G., Kawashita, K. and Reynolds, J.H. (1967) Potassium-argon ages of alkaline rocks from Southern Brazil. *Geochim. Cosmochim. Acta*, **31**, 117–142.
- Armenteros, I. and Huerta, P. (2006) The role of clastic sediment influx in the formation of calcrete and palustrine facies: a response to paleogeographic and climatic conditions in the southeastern Tertiary Duero basin (northern Spain). In: *Paleoenvironmental Record and Applications of Calcretes and Palustrine Carbonates* (Eds A.M. Alonso-Zarza and L.H. Tanner). *Geol. Soc. Am. Spec. Paper*, **416**, 119–132.
- Atchley, S.C., Nordt, L.C. and Dworkin, S.I. (2004) Eustatic control on alluvial sequence stratigraphy: a possible example from the K/T transition of the Tornillo Basin, Big Bend National Park, West Texas. *J. Sed. Res.*, **74**, 391–404.
- Barcelos, J.H. (1984) Reconstrução paleogeográfica da sedimentação do Grupo Bauru baseada na sua redefinição estratiográfica parcial em território Paulista e no estudo preliminar fora do Estado de São Paulo. Livre Docência Thesis, Geosciences and Exact Sciences Institute - UNESP, São Paulo State University. Rio Claro, São Paulo, 190 pp.
- Barison, M.R. (2003) Estudo hidrogeológico da porção meridional do sistema aquífero Bauru no Estado de São Paulo. Master Science Thesis. Geosciences and Exact Sciences Institute, São Paulo State University - UNESP. Rio Claro, São Paulo, 158 pp.
- Basilici, G., Dal'Bó, P.F. and Oliveira, E.F. (2016) Distribution of palaeosols and deposits in the temporal Evolution of a semi-arid fluvial distributive system (Bauru Group, Upper Cretaceous, SE Brazil). *Sed. Geol.*, **341**, 245–264.
- Batezelli, A. (1998) Redefinição Litoestratiográfica da Unidade Araçatuba e da sua Extensão Regional na Bacia Bauru no Estado de São Paulo. Master Science Thesis, Geosciences and Exact Sciences Institute, São Paulo State University - UNESP. Rio Claro, São Paulo, 110 pp.
- Batezelli, A. (2003) Análise da Sedimentação Cretácea no Triângulo Mineiro e sua Correlação com Áreas Adjacentes. PhD Thesis. Geosciences and Exact Sciences Institute, São Paulo State University - UNESP. Rio Claro, São Paulo, 183 pp.

- Batezelli, A.** (2010) Arcabouço tectono-estratigráfico e evolução das bacias Caiuá e Bauru no Sudeste brasileiro. *Braz. J. Geol.*, **40**, 265–285.
- Batezelli, A.** (2015) Continental systems tracts of the Brazilian Cretaceous Bauru Basin and their relationship with the tectonic and climatic evolution of South America. *Basin Res.*, **29**, 1–25.
- Batezelli, A., Gomes, N.S. and Perinotto, J.A.de.J.** (2005) Petrografia e Evolução Diagenética dos Arenitos da Porção Norte e Nordeste da Bacia Bauru (Cretáceo Superior). *Braz. J. Geol.*, **35**, 311–322.
- Batezelli, A. and Ladeira, F.S.B.** (2016) Stratigraphic framework and evolution of the Cretaceous continental sequences of the Bauru, Sanfranciscana, and Parecis basins, Brazil. *J. S. Am. Earth Sci.*, **65**, 1–24.
- Batezelli, A., Saad, A.R. and Basilici, G.** (2007) Arquitetura deposicional e evolução da seqüência aluvial neocretácea da porção setentrional da Bacia Bauru, no sudeste brasileiro. *Braz. J. Geol.*, **37**, 163–181.
- Birkeland, P.W.** (1999) *Soils and Geomorphology*. Oxford Univ. Press, New York, 430 pp.
- Bown, T.M. and Kraus, M.J.** (1987) Integration of channel and floodplain suites in aggrading fluvial systems. I. Developmental sequence and lateral relations of lower Eocene alluvial palaeosols, Willwood Formation, Bighorn Basin, Wyoming. *J. Sed. Petrol.*, **57**, 587–601.
- Buol, S.W., Southard, R.J., Graham, R.C. and McDaniel, P.A.** (2011) *Soil Genesis and Classification*. Iowa State University Press, Iowa City, IA, 543 pp.
- Cain, S.A. and Mountney, N.P.** (2009) Spatial and temporal evolution of a terminal fluvial fan system: the Permian Organ Rock Formation, south-east Utah, USA. *Sedimentology*, **56**, 1774–1800.
- Candy, I. and Black, S.** (2009) The timing of Quaternary calcrete development in semi-arid southeast Spain: investigating the role of climate on calcrete genesis. *Sed. Geol.*, **218**, 6–15.
- Candy, I., Black, S., Sellwood, B.W. and Rowan, J.S.** (2003) Calcrete profile development in Quaternary alluvial sequences, southeast Spain: implications for using calcretes as a basis for landform chronologies. *Earth Surf. Proc. Land.*, **28**, 169–185.
- Candy, I., Black, S. and Sellwood, B.W.** (2004) Quantifying time scales of pedogenic calcrete formation using U-series disequilibria. *Sed. Geol.*, **170**, 177–187.
- Capilla, R.** (2002) A Formação Marília (Cretáceo Superior) na Região de Uberaba (MG), uma Nova Interpretação. In: CONGRESSO BRASILEIRO DE GEOLOGIA, XLI, João Pessoa (PB). Anais. . João Pessoa (PB), SBG, 378 pp.
- Cecil, C.B.** (1990) Paleoclimate controls on stratigraphic repetition of chemical and siliciclastic rocks. *Geology*, **18**, 533–536.
- Cecil, C.B.** (2003). The concept of autocyclic and allocyclic controls on sedimentation and stratigraphy, emphasizing the climatic variable. In: *Climate Controls on Stratigraphy* (Eds C.B. Cecil and T.N. Edgar), *SEPM Spec. Publ.*, **77**, 13–20.
- Cecil, C.B.** (2013) An overview and interpretation of autocyclic and allocyclic processes and the accumulation of strata during the Pennsylvanian-Permian transition in the central Appalachian Basin, USA. *Int. J. Coal Geol.*, **119**, 21–31.
- Chen, X.Y. and Eggleton, R.A.** (2002) Mineralogy and chemistry. In: *Calcrete: Characteristics, Distribution and Use in Mineral Exploration* (Eds J. Lintern, I. Roach and X.Y. Chen), pp. 23–30. Instant Colour Press, Belconnen.
- Cleveland, D.M., Atchley, S.C. and Nordt, L.C.** (2007) Continental Sequence Stratigraphy of the Upper Triassic (Norian–Rhaetian) Chinle Strata, Northern New Mexico, U.S.A.: Allocyclic and Autocyclic Origins of Palaeosol-Bearing Alluvial Successions. *J. Sed. Res.*, **77**, 909–924.
- Coimbra, A.M.** (1991) Sistematização Crítica da Obra. Livredocência Thesis, Instituto de Geociências da Universidade de São Paulo, 54 pp.
- Coimbra, A.M., Brandt Neto, M. and Coutinho, J.M.V.** (1981) Silicificação dos Arenitos da Formação Bauru no Estado de São Paulo. In: *A Formação Bauru no Estado de São Paulo e Regiões Adjacentes* (Ed. SBG), pp. 103–115. Coletânea de trabalhos e debates, São Paulo.
- Colson, J., Cojan, I. and Thiry, M.** (1998) A hydrogeological model for palygorskite formation in the Danian continental facies of the Provence Basin (France). *Clays Minerals*, **33**, 333–347.
- Currie, B.S., Colombi, C.E., Tabor, N.J., Shipman, T.C. and Montañez, I.P.** (2009) Stratigraphy and architecture of the Upper Triassic Ischigualasto Formation, Ischigualasto Provincial Park, San Juan, Argentina. *J. S. Am. Earth Sci.*, **27**, 74–87.
- Currie, B.S.** (1998) Upper Jurassic-Lower Cretaceous Morrison and Cedar Mountain Formations, northeastern Utah-northwestern Colorado: relationships between nonmarine deposition and Early Cordilleran foreland-basin development. *J. Sed. Res.*, **68**, 632–652.
- Dal’Bo, P.F.F., Basilici, G., Angelica, R.S. and Ladeira, F.S.B.** (2009) Paleoclimatic interpretations from pedogenic calcretes in a Maastrichtian semi-arid eolian sand-sheet paleoenvironment: Marília Formation (Bauru Basin, southeastern Brazil). *Cretac. Res.*, **30**, 659–675.
- Daoudi, L.** (2004) Palygorskite in the uppermost Cretaceous-Eocene Rocks from Marrakech high Atlas, Morocco. *J. Afr. Earth Sci.*, **39**, 353–358.
- Davidson, S.K., Hartley, A.J., Weissmann, G.S., Nichols, G.J. and Scuderi, L.A.** (2013) Geomorphic elements on modern distributive fluvial systems. *Geomorphology*, **180–181**, 82–95.
- DeCelles, P.G. and Cavazza, W.** (1999) A comparison of fluvial megafans in the Cordilleran (Upper Cretaceous) and modern Himalayan foreland basin systems. *Geol. Soc. Am. Bull.*, **111**, 1315–1334.
- De la Horra, R., Benito, M.I., López-Gómez, J., Arche, A., Barrenechea, J.F. and Luque, F.J.** (2008) Paleoenvironmental significance of Late Permian palaeosols in the SE Iberian Ranges, Spain. *Sedimentology*, **55**, 1849–1873.
- Demko, T.M., Currie, B.S. and Nicoll, K.A.** (2004) Regional paleoclimatic and stratigraphic implications of palaeosols and fluvial/overbank architecture in the Morrison Formation (Upper Jurassic), Western Interior, USA. *Sed. Geol.*, **167**, 115–135.
- Dias-Brito, D., Musacchio, E.A., Castro, J.C., Maranhão, M.S.A.S., Suárez, J.M. and Rodrigues, R.** (2001) Grupo Bauru: uma unidade continental cretácea no Brasil – concepções baseadas em dados micropaleontológicos, isotópicos e estratigráficos. *Rev. Paléobiol. Genève*, **20**, 245–304.
- Durand, N., Monger, H.C. and Canti, M.G.** (2010) Calcium carbonate features. In: *Interpretation of Micromorphological Features in Soils and Regoliths* (Eds G. Stoops, V. Marcelino and F. Mees), pp. 149–194. Elsevier, Amsterdam, the Netherlands.

- Eberth, D.A.** and **Miall, A.D.** (1991) Stratigraphy, sedimentology and evolution of vertebrate-bearing, braided to anastomosed fluvial systems, Cuttler Formation (Permian to Pennsylvanian), north-central New Mexico. *Sed. Geol.*, **72**, 225–252.
- Etchebehere, M.L., De, C., Saad, A.R., Taddeo, J.S.** and **Hellmeister Jr, Z.** (1991) Moldes de cristais salinos no Grupo Bauru, estado de São Paulo: Implicações econômicas e paleoclimáticas. *Rev. Geociênc.*, **10**, 101–117.
- Fedoroff, N.** and **Courty, M.A.** (1989) Indicateurs pédogéniques d'aridification. In: Exemple du Sahara. *Bulletin de la Société géologique de France*. Séance spécialisée, Sahara, pp. 43–53.
- Fernandes, L.A.** (1998) Estratigrafia e Evolução Geológica da Parte Oriental da Bacia Bauru (Ks, Brasil). PhD Thesis, Geoscience Institute, São Paulo University - USP, 216 pp.
- Fernandes, L.A.** (2010) Calcretes e registros de paleossolos em depósitos continentais neocretáceos (Bacia Bauru, Formação Marília). *Braz. J. Geol.*, **40**, 19–35.
- Fernandes, L.A.** and **Coimbra, A.M.** (2000) Revisão Estratigráfica da Parte Oriental da Bacia Bauru (Neocretáceo). *Braz. J. Geol.*, **30**, 717–728.
- Fernandes, L.A.** and **Ribeiro, C.M.M.** (2015) Evolution and palaeoenvironment of the Bauru Basin (upper Cretaceous, Brazil). *J. S. Am. Earth Sci.*, **61**, 71–90.
- Fisher, J.A., Nichols, G.J.** and **Waltham, D.A.** (2007) Unconfined flow deposits in distal sectors of fluvial distributary systems: examples from the Miocene Luna and Huesca Systems, northern Spain. *Sed. Geol.*, **195**, 55–73.
- Fragoso, C.E., Weinschütz, L.C., Vega, C.S., Guimarães, G.B., Manzig, P.C.** and **Kellner, A.W.A.** (2013) Short note on the pterosaurs from the Caiuá Group (Upper Cretaceous, Bauru Basin), Paraná State, Brazil. In: Rio Pterio 2013 - International Symposium on Pterosaurs, 2013, Rio de Janeiro. International Symposium on Pterosaurs, Short Communications, 71–72.
- Friend, P.F.** (1983) Towards the field classification of alluvial architecture or sequence. In: *Modern and Ancient Fluvial Systems* (Eds J.D. Collinson and J.L. Lewin), *Spec. Publ. Int. Ass. Sed.*, **6**, 345–354.
- Fulfaro, V.J.** (1974) Tectônica do Alinhamento Estrutural do Paranapanema. *Geosci. Inst. Bull. São Paulo Univ. USP*, **5**, 129–138.
- Fulfaro, V.J., Perinotto, J.A.J.** and **Barcelos, J.H.A.** (1994) Margem Goiana de Grupo Bauru: Implicações na Litoestratigrafia e Paleogeografia. In: Simpósio Sobre o Cretáceo do Brasil, 3, Rio Claro (SP), Brasil. Boletim. Rio Claro, Unesp. pp. 81–84.
- Fulfaro, V.J.** and **Perinotto, J.A.J.** (1996) A Bacia Bauru: estado da arte. In: Boletim do 4 Simpósio sobre o Cretáceo do Brasil, pp. 297–303.
- Galán, E.** and **Pozo, M.** (2011) Palygorskite and sepiolite deposits in continental environments. Description, genetic patterns and sedimentary settings. In: *Developments in Palygorskite-Sepiolite Research: a New Outlook on These Nanomaterials* (Eds E. Galan and A. Singer), pp. 125–176. Elsevier, Amsterdam.
- Galloway, W.E.** and **Hobday, D.K.** (1983) *Terrigenous Clastic Depositional Systems – Applications to Petroleum, Coal, and Uranium Exploration*. Springer-Verlag, New York, 423 pp.
- Geddes, A.** (1960) The alluvial morphology of the Indo-Gangetic Plain: its mapping and geographical significance. *Trans. Pap. Inst. Br. Geogr.*, **28**, 253–276.
- Gibling, M.R.** (2006) Width and thickness of fluvial channel bodies and valley fills in the geological record: a literature compilation and classification. *J. Sed. Res.*, **76**, 731–770.
- Gibson, S.A., Thompson, R.N., Leonardos, O.H., Dickin, A.P.** and **Mitchell, J.G.** (1995) The Late Cretaceous Impact of the Trindade Mantle Plume: Evidence From Large Volume, Mafic, Potassic Magmatism in SE Brazil. *J. Petrol.*, **36**, 189–229.
- Gile, L.H.** (1975) Holocene soils and soil-geomorphic relations in an arid region of Southern New Mexico. *Quatern. Res.*, **5**, 321–360.
- Gobbo-Rodrigues, S.R.** (2001) Carófitas e Ostrácodos do Grupo Bauru. Master Science Thesis, Geosciences and Exact Sciences Institute, São Paulo State University - UNESP. Rio Claro, São Paulo, 137 pp.
- Gocke, M., Pustovoytov, K.** and **Kuzyakov, Y.** (2012) Pedogenic carbonate formation: recrystallization versus migration—process rates and periods assessed by <sup>14</sup>C labeling. *Global Biogeochemical Cycles* **26**.
- Goudie, A.S.** (1983) Calcrete. In: *Chemical Sediments and Geomorphology* (Eds A.S. Goudie and K. Pye), pp. 93–131. Academic Press, London.
- Guimarães, G.B., Icardo, A., Godoy, L.C., Weinschütz, L.C., Manzig, P.C., Vega, C.S.** and **Pilatti, F.** (2012) Ocorrência de Pterossauros no Cretáceo da Bacia do Paraná/Bauru: Implicações para a Geoconservação, Paleontologia e Estratigrafia. In: 46th Geology Brazilian Congress, Santos (São Paulo), 48.
- Hampton, B.A.** and **Horton, B.K.** (2007) Sheet flow fluvial processes in a rapidly subsiding basin, Altiplano plateau, Bolivia. *Sedimentology*, **54**, 1121–1147.
- Hanneman, D.L.** and **Wideman, C.J.** (2010) Continental sequence stratigraphy and continental carbonates. In: *Carbonates in Continental Settings: Geochemistry, Diagenesis and Applications Developments in Sedimentology* (Eds M. Alonso-Zarza and L.H. Tanner), pp. 215–273. Elsevier, Amsterdam.
- Hartley, A.J.** (1993) A depositional model for the Mid-Westphalian A to late Westphalian B Coal Measures of South Wales. *J. Geol. Soc.*, **150**, 1121–1136.
- Hartley, A.J., Weissmann, G.S., Bhattacharayya, P., Nichols, G.J., Scuderi, L.A., Davidson, S.K., Leleu, S., Chakraborty, T., Gosh, P.** and **Mather, A.E.** (2012) Soil development on modern distributive fluvial systems: preliminary observations with implications for interpretation of palaeosols in the rock record. In: *New Frontiers in Paleopedology and Terrestrial Paleoclimatology. Palaeosols and Soil Surface Analog Systems* (Eds S.G. Driese and L.C. Nordt). *SEPM Spec. Publ.*, **104**, 149–158.
- Hartley, A.J., Weissmann, G.S., Bhattacharayya, P., Nichols, G.J., Scuderi, L.A., Davidson, S.K., Leleu, S., Chakraborty, T., Ghosh, P.** and **Mather, A.E.** (2013) Soil development on modern distributive fluvial systems: preliminary observations with implications for interpretation of palaeosols in the rock record. In: *New Frontiers in Paleopedology and Terrestrial Paleoclimatology* (Ed. S. Driese), *SEPM Spec. Publ.*, **104**, 149–158.
- Hartley, A.J., Weissmann, G.S., Nichols, G.J.** and **Warwick, G.L.** (2010) Large distributive fluvial systems: characteristics, distribution, and controls on development. *J. Sed. Res.*, **80**, 167–183.
- Hasui, Y.** and **Cordani, U.G.** (1968) Idades potássio-argônio de rochas eruptivas mesozóicas do oeste mineiro e sul de Goiás. In: 2nd Brazilian Geology Congress Boletim, Belo Horizonte, pp. 139–143.

- Hasui, Y. and Haralyi, N.L.E.** (1991) Aspectos Lito-estruturais e Geofísicos do Soerguimento do Alto Paranaíba. *Rev. Geociênc.*, **10**, 67–77.
- Herrero, J., Porta, J. and Fedoroff, N.** (1992) Hypergypsic soil micromorphology and landscape relationships in north eastern Spain. *Soil Sci. Soc. Am. J.*, **56**, 1188–1194.
- Hirst, J.P.P.** (1991) Variations in alluvial architecture across the Oligo-Miocene Huesca fluvial system, Ebro Basin, Spain. In: *The Three Dimensional Facies Architecture of Terrigenous Clastic Sediments and Its Implications for Hydrocarbon Discovery and Recovery* (Eds A.D. Miall and N. Tyler), *SEPM Concepts Sedimentol. Paleontol.* **3**, 111–121.
- Jaillard, B., Guyon, A. and Maurin, A.F.** (1991) Structure and composition of calcified 834 roots, and their identification in calcareous soils. *Geoderma*, **50**, 197–210.
- Jie, Z. and Chafetz, H.S.** (2010) Pedogenic Carbonates in Texas: stable-Isotope Distributions and their Implications for Reconstructing Region-Wide Paleoenvironments. *J. Sed. Res.*, **80**, 137–150.
- Jones, S.J., Frostick, L.E. and Astin, T.R.** (2001) Braided Stream and Flood Plain Architecture: the Rio Vero Formation, Spanish Pyrenees. *Sed. Geol.*, **139**, 229–260.
- Kabanov, P.B., Alekseeva, T.V., Alekseeva, V.A., Alekseev, A.O. and Gubin, S.** (2010) Palaeosols in Late Moscovian (Carboniferous) Marine Carbonates of the East European Craton Revealing “Great Calcimagnesian Plain” Paleolandscapes. *J. Sed. Res.*, **80**, 195–215.
- Kelly, S.B. and Olsen, H.** (1993) Terminal fans: a review with reference to Devonian examples. *Sed. Geol.*, **85**, 339–374.
- Khadkikar, A.S., Merh, S.S., Malik, J.N. and Chamyal, L.S.** (1998) Calcretes in semi-arid alluvial systems: formative pathways and sinks. *Sed. Geol.*, **116**, 251–260.
- Khadkikar, A.S., Chamyal, L.S. and Ramesh, R.** (2000) The character and genesis of calcrete in Late Quaternary alluvial deposits, Gujarat, western India, and its bearing on the interpretation of ancient climates. *Palaeogeogr. Palaeoclimatol. Palaeoecol.*, **162**, 239–261.
- Khormali, F., Abtahi, A., Mahmoodi, S. and Stoops, G.** (2003) Argillic horizon development in calcareous soils of arid and semi-arid regions of southern Iran. *Catena*, **53**, 273–301.
- Klappa, C.F.** (1978) Biolithogenesis of Microcodium: elucidation. *Sedimentology*, **25**, 489–522.
- Klappa, C.F.** (1980) Rhizoliths in terrestrial carbonates: classification, recognition, genesis, and significance. *Sedimentology*, **26**, 613–629.
- Klappa, C.F.** (1983) A process-response model for the formation of pedogenic calcretes. In: *Residual Deposits: Surface Related Weathering Processes and Materials* (Ed. R.C.L. Wilson), pp. 211–220. *Geol. Soc. Spec. Public.* Blackwell Scientific Publications, Oxford.
- Kosir, A.** (2004) Microcodium revisited: root calcification products of terrestrial plants on carbonate-rich substrates. *J. Sed. Res.*, **74**, 845–857.
- Kraus, M.** (1999) Palaeosols in clastic sedimentary rocks: their geologic applications. *Earth Sci. Rev.*, **47**, 41–70.
- Kraus, M.J.** (2002) Basin-scale changes in floodplain palaeosols: implications for interpreting alluvial architecture. *J. Sed. Res.*, **72**, 500–509.
- Kraus, M.J. and Hasiotis, S.T.** (2006) Significance of different modes of rhizolith preservation to interpreting paleoenvironmental and paleohydrologic settings: examples from Paleogene palaeosols, Bighorn Basin, Wyoming, U.S.A. *J. Sed. Res.*, **76**, 633–646.
- Kraus, M.J., McInerney, F.A., Wing, S.L., Secord, R., Baczynski, A.A. and Bloch, J.I.** (2013) Paleohydrologic response to continental warming during the Paleocene-Eocene Thermal Maximum, Bighorn Basin, Wyoming. *Palaeogeogr. Palaeoclimatol. Palaeoecol.*, **370**, 196–208.
- Leier, A.L., DeCelles, P.G. and Pelletier, J.D.** (2005) Mountains, monsoons, and megafans. *Geology*, **33**, 289–292.
- Ladeira, F.S.B., Basilici, G., Dal’Bo, P.F.F. and Brolesi, M.F.** (2008) Paleossolos da Formação Marília: contribuição à reconstituição paleogeográfica cretácica na porção norte da Bacia Sedimentar do Paraná - (Quirinópolis e Itajá-GO). *Geogr. Ensino Pesquisa*, **12**, 4807–4818.
- Lepsch, I.F., Moniz, A.C. and Rotta, C.L.** (1977) Evolução mineralógica de solos derivados da Formação Bauru em Echaporã, São Paulo. *Rev. Brasil. Ciênc. Solo*, **1**, 38–43.
- Lintern, M.J.** (2015) The association of gold with calcrete. *Ore Geol. Rev.*, **66**, 132–199.
- Machado Junior, D.L.** (1992) Idades Rb/Sr do complexo alcalino-carbonatítico de Catalão II (GO). In: 29th Brazilian Geology Congress Bulletin, São Paulo, Brazil, 91–93.
- Mack, G.H. and Madoff, R.D.** (2005) A test of models of fluvial architecture and palaeosol development: Camp Rice Formation (Upper Pliocene-Lower Pleistocene), southern Rio Grande rift, New Mexico, USA. *Sedimentology*, **52**, 191–211.
- Machette, M.N.** (1985) Calcic soils of southwestern United States. In: *Soil and Quaternary Geology of the Southwestern United States* (Ed. D.L. Weide), *Geol. Soc. Am. Spec. Paper* **203**, 1–21.
- Marriott, S.B. and Wright, V.P.** (1993) Palaeosols as indicators of geomorphic stability in two Old Red Sandstone alluvial suites, South Wales. *J. Geol. Soc. London*, **150**, 1109–1120.
- Martinelli, A.G., Riff, D. and Lopes, R.P.** (2011) Discussion about the occurrence of the genus *Aeolosaurus* Powell 1987 (Dinosauria, Titanosauria) in the Upper Cretaceous of Brazil. *GAEA J. Geosci. Unisinos*, **7**, 34–40.
- McBride, E.F.** (1963) A classification of common sandstones. *J. Sed. Petrol.*, **33**, 664–669.
- McCarthy, P.J. and Plint, A.G.** (2003) Spatial variability of palaeosols across Cretaceous interfluvies in the Dunvegan Formation, NE British Columbia, Canadá; palaeohydrological, palaeogeomorphological and stratigraphic implications. *Sedimentology*, **50**, 1187–1220.
- McCarthy, P.J., Martini, I.P. and Leckie, D.A.** (1997) Anatomy and evolution of a Lower Cretaceous alluvial plain: sedimentology and palaeosols in the upper Blairmore Group, south-western Alberta, Canada. *Sedimentology*, **44**, 197–220.
- McCarthy, P.J., Faccini, U.F. and Plint, A.G.** (1999) Evolution of an ancient coastal plain: palaeosols, interfluvies and alluvial architecture in a sequence stratigraphic framework, Cenomanian Dunvegan Formation, NE British Columbia, Canada. *Sedimentology*, **46**, 861–891.
- McFadden, L.D. and Tinsley, J.C.** (1985) Rate and depth of pedogenic-carbonate accumulation in soils: formulation and testing of a compartment model. In: *Soil and Quaternary Geology of the Southwestern United States* (Ed. D.L. Weide), *Geol. Soc. Am.*, 545 pp.
- Meléndez, A., Alonso-Zarza, A.M. and Sancho, C.** (2011) Multistorey calcrete profiles developed during the initial stages of the configuration of the Ebro basin’s exorheic fluvial network. *Geomorphology*, **134**, 232–248.

- Miall, A.D.** (1985) Architectural-Element Analysis: a New Method of Facies Analysis Applied to Fluvial Deposits. *Earth-Sci. Rev.*, **22**, 261–300.
- Miall, A.D.** (1996) *The Geology of Fluvial Deposits*. Springer-Verlag, Berlin, Germany, 582 pp.
- Miall, A.D.** (2010) The Geology of stratigraphic sequences. Springer Science & Business Media, 522 pp.
- Miall, A.D.** and **Jones, B.G.** (2003) Fluvial architecture of the Hawkesbury Sandstone (Triassic), near Sydney, Australia. *J. Sed. Res.*, **73**, 531–545.
- Mitchum Jr, R.M., Vail, P.R.** and **Thompson III, S.** (1977) Seismic Stratigraphy and Global Changes of Sea Level, Part 2: The depositional sequence as a basic unit for stratigraphy analysis. In: *Seismic Stratigraphy – Applications to Hydrocarbon Exploration* (Ed. C.E. Payton), *Am. Assoc. Petrol. Geol. Memoir.*, **26**, 516.
- Mohindra, R., Parkash, B.** and **Prasad, J.** (1992) Historical geomorphology and pedology of the Gandak Megafan, Middle Gangetic Plains, India. *Earth Surf. Proc. Land.*, **17**, 643–662.
- Nascimento, D.L., Ladeira, F.S.B.** and **Batezelli, A.** (2017) Pedodiagenetic Characterization of Cretaceous Palaeosols in Southwest Minas Gerais, Brazil. *Revista Brasileira de Ciência do Solo*, **41**.
- Nash, D.J.** and **Smith, R.F.** (1998) Multiple calcrete profiles in the Tabernas Basin, SE Spain: their origins and geomorphic implications. *Earth Surf. Proc. Land.*, **23**, 1009–1029.
- Nash, D.J.** and **McLaren, S.J.** (Eds) (2003) *Geochemical Sediments and Landscapes*. Blackwell, Oxford, 10–45 pp.
- Nichols, G.J.** and **Fisher, J.A.** (2007) Processes, facies and architecture of fluvial distributary system deposits. *Sed. Geol.*, **195**, 75–90.
- Owen, A., Nichols, G.J., Hartley, A.J., Weissmann, G.S.** and **Scuderi, L.A.** (2015) Quantification of a distributive fluvial system; The salt Wash DFS of the Morrison Formation, SW USA. *J. Sed. Res.*, **85**, 544–561.
- Owen, A., Nichols, G.J., Hartley, A.J.** and **Weissmann, G.S.** (2017) Vertical trends within the prograding Salt Wash distributive fluvial system, SW United States. *Basin Res.*, **2015**, 1–17.
- Paulae Silva, F., Chang, H.K.** and **Caetano-Chang, M.R.** (2005) Estratigrafia de subsuperfície do Grupo Bauru (K) no Estado de São Paulo. *Rev. Brasil. Geociênc.*, **35**, 77–88.
- Pereira, C.T., Batezelli, A.** and **Ladeira, F.S.B.** (2015) Paleoprecipitation changes based on palaeosols profiles of the Marília Formation (Upper Cretaceous) in the eastern portion of the Bauru Basin in Southeastern Brazil. *Geociências*, **34**, 238–257.
- Pimentel, N.L., Wright, V.P.** and **Azevedo, T.M.** (1996) Distinguishing early groundwater alteration effects from pedogenesis in ancient alluvial basins: examples from the Palaeogene of Portugal. *Sed. Geol.*, **105**, 1210. Special Paper 203, pp. 23–41.
- Plaziat, J.C.** and **Freytet, P.** (1978) Le pseudo-microkarst pédologique: un aspect particulier des paléo-pédogenèses développées sur les dépôts calcaires lacustres dans le tertiaire du Languedoc. *CR Acad. Sci. Paris*, **286**, 1661–1664.
- Prochnow, S.J., Nordt, L.C., Atchley, S.C.** and **Hudec, M.R.** (2006) Multi-proxy palaeosol evidence for middle and late Triassic climate trends in eastern Utah. *Palaeogeogr. Palaeoclimatol. Palaeoecol.*, **232**, 53–72.
- Posamentier, H.W.** and **Allen, G.P.** (1999) Siliciclastic sequence stratigraphy: concepts and applications. *SEPM Concepts Sed. Paleontol.*, **7**, 210.
- Santucci, R.M.** and **Bertini, R.J.** (2001) Distribuição Paleogeográfica e Biocronológica dos Titanossauros (Saurishia, Sauropoda) do Grupo Bauru, Cretáceo Superior do Sudeste Brasileiro. *Braz. J. Geol.*, **31**, 307–315.
- Ramos, A.** and **Sopeña, A.** (1983) Gravel Bars in Low-Sinuosity Streams (Permian and Triassic, Central Spain). In: *Modern and Ancient Fluvial Systems* (Eds J.D. Collinson and J. Lewis), *Int. Assoc. Sediment. Spec. Publ.*, **6**, 301–312.
- Retallack, G.J.** (2001) *Soils of the Past: an introduction to paleopedology*, 2nd edn, pp. 404. Blackwell Science, Oxford.
- Ribeiro, D.T.P.** (2000) Caracterização dos Silcretos do Membro Serra da Galga, Formação Marília, Grupo Bauru na Região do Triângulo Mineiro. *Braz. J. Geol.*, **30**, 663–664.
- Ribeiro, D.T.P.** (2001) Diagênese das Rochas do Membro Serra da Galga, Formação Marília, Grupo Bauru (Cretáceo da Bacia do Paraná), na Região de Uberaba, Minas Gerais. *Braz. J. Geol.*, **31**, 7–12.
- Riccomini, C.** (1997) Arcabouço Estrutural e Aspectos do Tectonismo Gerador e Deformador da Bacia Bauru no Estado de São Paulo. *Braz. J. Geol.*, **27**, 153–162.
- Schoeneberger, P.J., Wysocki, D.A.** and **Benham, E.C.**, Soil Survey Staff (2012) Field Book for Describing and Sampling Soils, Version 3.0. Natural Resources Conservation Service, National Soil Survey Center, Lincoln, NE, pp. 9–14.
- Sheldon, N.D.** and **Tabor, N.J.** (2009) Quantitative paleoenvironmental and paleoclimatic reconstruction using palaeosols. *Earth Sci. Rev.*, **95**, 1–52.
- Shukla, U.K., Singh, I.B., Sharma, M.** and **Sharma, S.** (2001) A model of alluvial megafan sedimentation: Ganga megafan. *Sed. Geol.*, **144**, 243–262.
- Silva, M.L., Batezelli, A.** and **Ladeira, F.S.B.** (2015) Índices de intemperismo e evolução dos paleossolos da Formação Marília, Maastrichtiano da Bacia Neocretácea Bauru. *Geochim. Brasiliensis*, **29**, 127–138.
- Silva, M.L., Batezelli, A.** and **Ladeira, F.S.B.** (2016) Uso de estimativas de paleoprecipitação e paleotemperatura em paleossolos cretáceos no Brasil: abordagem crítica. *Geochim. Brasiliensis*, **30**, 72–83.
- Silva, M.L., Batezelli, A.** and **Ladeira, F.S.B.** (2017a) Micromorphology of palaeosols of the Marília Formation and their significance in the paleoenvironmental evolution of the Bauru Basin, Upper Cretaceous, southeastern Brazil. *Revista Brasileira de Ciência do Solo*, **41**, e0160287.
- Silva, M.L., Batezelli, A.** and **Ladeira, F.S.B.** (2017b) The mineralogy of palaeosols in the Marília Formation and their importance in the environmental evolution of the Maastrichtian of the Bauru Basin in southeastern Brazil. *Braz. J. Geol.*, **47**, 403–426.
- Silva, M.L., Batezelli, A.** and **Ladeira, F.S.B.** (2017c) Genesis and paleoclimatic significance of palygorskite in the cretaceous palaeosols of the Bauru Basin, Brazil. *Catena*, **168**, 110–128. <https://doi.org/10.1016/j.catena.2017.12.031>.
- Singh, H., Parkash, B.** and **Gohain, K.** (1993) Facies analysis of the Kosi megafan deposits. *Sed. Geol.*, **85**, 87–113.
- Smith, J.J., Hasiotis, S., Woody, D.T.** and **Kraus, M.J.** (2008) Paleoclimatic Implications of Crayfish-Mediated Prismatic Structures in Palaeosols of the Paleogene Willwood Formation, Bighorn Basin, Wyoming, U.S.A. *J. Sed. Res.*, **78**, 323–334.
- Soares, M.V.T., Basilici, G., DalBó, P.F., Marinho, T.S., Mountney, N.P., Colombera, L., Oliveira, E.F.** and **Silva,**

- K.E.B.** (2018) Climatic and geomorphologic cycles in a semiarid distributive fluvial system, Upper Cretaceous, Bauru Group, SE Brazil. *Sed. Geol.*, **372**, 75–95.
- Soil Survey Staff (2006) *Keys to Soil Taxonomy*, 10th edn. US Department of Agriculture, Natural Resource Conservation Service, Washington DC, 332 pp.
- Sonoki, I.K. and Garda, G.M.** (1988) Idades K-Ar de rochas alcalinas do Brasil Meridional e Paraguai Oriental: compilação e adaptação às novas constantes de decaimento. *Geosci. Inst. Bull. São Paulo Univ. USP Cientific Ser.*, **19**, 63–85.
- Stanistreet, I.G. and McCarthy, T.S.** (1993) The Okavango Fan and the classification of sub aerial fan systems. *Sed. Geol.*, **85**, 115–133.
- Steila, D.** (1976) *The Geography of Soils*. Prentice-Hall, Upper Saddle River, NJ, 222 pp.
- Stoops, G., Marcelino, V. and Mees, F.** (2010) *Interpretation of Micromorphological Features of Soils and Regoliths*. Elsevier, Amsterdam.
- Suguo, K. and Barcelos, J.H.** (1983) Calcretes of the Bauru Group (Cretaceous), Brazil: petrology and geological significance. *Boletim do Instituto de Geociências da Universidade de São Paulo*, **14**, 31–47.
- Suguo, K., Berenholc, M. and Salati, E.** (1975) Composição Química e Isotópica dos Calcários e Ambiente de Sedimentação da Formação Bauru. *Geosci. Inst. Bull. Univ. São Paulo*, **6**, 55–75.
- Suguo, K., Fulfaro, V.J., Amaral, G. and Guidorzi, L.A.** (1977) Comportamentos Estratigráficos e Estrutural da Formação Bauru nas Regiões Administrativas 7 (Bauru), 8 (São José do Rio Preto) e 9 (Araçatuba) no Estado de São Paulo. In: SIMPÓSIO REGIONAL DE GEOLOGIA, 1, 1977, São Paulo. Atas... São Paulo: SBG, **2**, 231–247.
- Talbot, M.R.** (1985) Major bounding surfaces in eolian sandstones – a climatic model. *Sedimentology*, **32**, 257–265.
- Tabor, N.J. and Myers, T.S.** (2015) Palaeosols as indicators of paleoenvironment and paleoclimate. *Annu. Rev. Earth Planet. Sci.*, **43**, 333–361.
- Tabor, N.J., Montañez, I.P., Kelso, K.A., Currie, B., Shipman, T. and Colombi, C.** (2006) A Late Triassic soil catena: landscape and climate controls on paleosol morphology and chemistry across the Carnian-age Ischigualasto-Villa Union Basin, northwestern Argentina. *Geol. Soc. Am. Spec. Pap.*, **416**, 17–41.
- Tanner, L.H.** (2010) Continental carbonates as indicators of paleoclimate. In: *Carbonates in Continental Settings: Geochemistry, Diagenesis and Applications* (Eds L.H. Tanner and A.M. Alonso-Zarza), pp. 179–214. Elsevier, Amsterdam.
- Trendell, A.M., Atchley, S.C. and Nordt, L.C.** (2013) Facies Analysis of a Probable Large-Fluvial-Fan Depositional System: The Upper Triassic Chinle Formation at Petrified Forest National Park, Arizona, U.S.A. *J. Sed. Res.*, **83**, 873–895.
- Weissmann, G.S., Hartley, A.J., Nichols, G.J., Scuderi, L.A., Olson, M., Buehler, H. and Banteah, R.** (2010) Fluvial form in modern continental sedimentary basins: distributive fluvial Systems. *Geology*, **38**, 39–42.
- Weissmann, G.S., Hartley, A.J., Scuderi, L.A., Nichols, G.J., Davidson, S.K., Owen, A., Atchley, S.C., Bhattacharyya, P., Chakraborty, T., Ghosh, P., Nordt, L.C., Michel, L. and Tabor, N.J.** (2013) Prograding distributive fluvial systems - geomorphic models and ancient examples. In: *New Frontiers in Paleopedology and Terrestrial Paleoclimatology* (Eds S.G. Dreise, L.C. Nordt and P.L. McCarthy), *SEPM Spec. Pub.*, **104**, 131–147.
- Wells, N.A. and Dorr, J.A.J.** (1987) A reconnaissance of sedimentation on the kosi alluvial fan of India. In: *Recent Developments in Fluvial Sedimentology* (Eds F.G. Ethridge, R.M. Flores and M.D. Harvey), *SEPM Spec. Publ.*, **39**, 51–61.
- Wright, V.P.** (1986) Palaeosols: their recognition and interpretation. In: *Princeton Series in Geology and Paleontology*, Princeton University Press, Princeton, NJ, 340 pp.
- Wright, V.P. and Tucker, M.E.** (1991) *Calcretes*, p. 352. Blackwell Scientific Publications, Carlton.
- Wright, V.P. and Marriott, S.B.** (1993) The sequence stratigraphy of fluvial depositional systems: the role of floodplain sediment storage. *Sed. Geol.*, **86**, 203–210.
- Wright, V.P.** (2007) Calcrete. In: *Geochemical Sediments and Landscapes* (Eds D.J. Nash and S.J. McLaren), pp. 10–45. Blackwell, Oxford.
- Wright, V.P., Platt, N.H., Marriott, S.B. and Beck, V.H.** (1995) A classification of rhizogenic (root-formed) calcretes. with examples from the Upper Jurassic-Lower Cretaceous of Spain and Upper Cretaceous of southern France. *Sed. Geol.*, **100**, 143–158.
- Zaleha, M.J.** (1997) Siwalik palaeosols (Miocene, northern Pakistan): genesis and controls on their formation. *J. Sed. Res.*, **67**, 821–839.
- Zamanian, K., Pustovoytov, K. and Kuzyakov, Y.** (2016) Pedogenic carbonates: forms and formation processes. *Earth Sci. Rev.*, **157**, 1–17.

*Manuscript received 21 August 2017; revision accepted 12 June 2018*